Eur Respir J 2002; 19: 722–742
DOI: 10.1183/09031936.02.00280002

European Respiratory Journal
ISSN 0903-1936

SERIES "CONTRIBUTIONS FROM THE EUROPEAN RESPIRATORY MONOGRAPH"
Edited by M. Decramer and A. Rossi
Number 7 in this Series

Diagnostic imaging of lung cancer

N. Hollings, P. Shaw

Diagnostic imaging of lung cancer. N. Hollings, P. Shaw. ©ERS Journals Ltd 2002.

ABSTRACT: Carcinoma of the bronchus is the most common malignancy in the Western world. It is also the leading cause of cancer-related death accounting for 32% of all cancer deaths in males and 25% in females [1]. In the USA it causes more deaths than cancers of the colon, breast and prostate combined [2]. Disappointingly, in a recent UK survey of improvements in cancer survival [3], carcinoma of the bronchus showed the smallest percentage reduction in the number of deaths avoided between 1981–1990 (0.2%). This compares badly with breast (11% reduction) and melanoma (32%). The overall 5-yr survival for lung cancer diagnosed between 1986–1990 was only 5.3% (against 66% for breast and 76% for melanoma). It is on this background that the radiologist remains actively employed in the detection, diagnosis, staging and review of this common malignancy.

Eur Respir J 2002; 19: 722–742.

Dept of Radiology, Cecil Fleming House, University College Hospital, Grafton Way, London, UK.

Correspondence: P. Shaw, Dept of Radiology, 2nd Floor, Cecil Fleming House, University College Hospital, Grafton Way, London, WC1E 6AV, UK.
Fax: 44 2073882147
E-mail: p.shaw@medphys.ucl.ac.uk

Keywords: Bronchial carcinoma, computed tomography, diagnostic imaging, magnetic resonance imaging, positron emission tomography, staging

Received: September 11 2001
Accepted September 11 2001

Lung cancer, in theory, should lend itself to screening. The disease is very common and in its earliest stages $\leqslant$70% of cases can be cured by surgery [4]. Despite this, lung cancer has an overall prognosis so dismal that incidence exceeds prevalence [5]. The main risk factor, smoking, is easily identifiable and noninvasive screening tests such as chest radiography and sputum cytology are widely available.

Why is screening not performed? Three large American screening programmes in the 1970s sponsored by the National Institute of Health [6–9] and another in Czechoslovakia in the 1980s [10] screened high-risk populations using chest radiography and sputum analysis. All showed increased detection of early-stage lung cancer, more resectable cancers and improved 5-yr survival rates in the screened *versus* control groups. Critically, however, none showed a statistically significant reduction in overall mortality.

In the last 5 yrs three nonrandomized trials incorporating low-dose computed tomography (CT) have reported prevalence screening data [11–13]. Their findings are summarized in (table 1). Also included in the table is preliminary data from two ongoing trials in the USA and Germany. These trials show that CT detects many more lung nodules than chest radiography. However, only a small percentage of these nodules turn out to be lung cancer. In the Mayo Clinic trial [7] for example, over one-half of all patients had at least one nodule. The logistics of differentiating benign from malignant nodules therefore becomes a very real issue and there have been concerns about the number of biopsies that may need to be performed. However, by assessment of patterns of calcification at both low-dose and high-resolution CT (HRCT) and repeat scanning after an interval, the Early Lung Cancer Action Project (ELCAP) group had only one incidence of biopsy performed for a benign, noncalcified nodule [11]. In this study, the cancer detection rate was 2.7% but it was $<$0.5% for the two other published studies (table 1). Although this seems low, it should be remembered that breast-cancer screening has a detection rate of only 0.6–0.7% [14].

The importance of rigorous study design cannot

Previous articles in this series: No. 1: Baldacci S, Omenaas E, Oryszcyn MP. Allergy markers in respiratory epidemiology. *Eur Respir J* 2001; 17: 773–790. **No. 2:** Antó JM, Vermeire P, Vestbo J, Sunyer J. Epidemiology of chronic obstructive pulmonary disease. *Eur Respir J* 2001; 17: 982–994. **No. 3:** Cuvelier A, Muir J-F. Noninvasive ventilation and obstructive lung diseases. *Eur Respir J* 2001; 17: 1271–1281. **No. 4:** Wysocki M, Antonelli M. Noninvasive mechanical ventilation in acute hypoxaemic respiratory failure. *Eur Respir J* 2001; 18: 209–220. **No. 5:** Østerlind K. Chemotherapy in small cell lung cancer. *Eur Respir J* 2001; 18: 1026–1043. **No. 6:** Jaakkola MS. Environmental tobacco smoke and health in the elderly. *Eur Respir J* 2002; 19: 172–181.

Table 1. – Data from low-dose computed tomography screening trials

	Patients n	Nodules %	Lung cancer incidence %
National Cancer Centre Hospital Japan [12]	1369	NA	15 (0.43)[#]
Shinshu University School of Medicine Japan [13]	3967	220 (5.6)	19 (0.35)
ELCAP USA [11]	1000	233 (23)	27 (2.7)
Mayo Clinic USA	1520	782 (51)	15 (1)
University of Münster Germany	919	NA	13 (1.4)

Data are presented as n (%) unless otherwise stated. ELCAP: Early Lung Cancer Action Project; NA: not available. [#]: represents percentage figure from 3,457 computed tomography examinations (in 1,369 patients).

be overemphasized when assessing the validity of these large and expensive trials. Although survival from the time of diagnosis of the disease is commonly reported it is not an appropriate measure of a diagnostic screening test and may be misleading as it is subject to lead-time bias, length-time bias and overdiagnosis bias. Change in mortality rather than survival is necessary to validate such screening methods [2]. Although low-dose CT can detect early stage disease 6–10 times more frequently than chest radiography [11, 15], there has not as yet been a similar fall in the prevalence of advanced disease [2]. This lack of so-called "stage shift" again questions the ability of low-dose CT screening to decrease overall mortality. Cross-contamination between the screened and control arms of the study is also a problem in these large trials, especially as the public at large become more aware of health issues. Individuals in the control-arm trials may worry that they are missing out on optimal treatment and manoeuvre their way into the screened population.

In an attempt to overcome these various difficulties, groups sponsored by the Medical Research Council in the UK and the National Cancer Institute in the USA are currently piloting prospective, randomized, controlled trials of 40,000 and 88,000 patients respectively using low-dose CT. The latter should have the power to detect a 20% reduction in mortality [2].

Radiological characteristics by cell type

Adenocarcinoma

Adenocarcinoma represents 31% of all lung cancers, including bronchoalveolar carcinoma [16]. Adenocarcinomas are typically peripherally located and measure <4 cm in diameter [17]; only 4% show cavitation [18]. Hila or hila and mediastinal involvement is seen in 51% of cases on chest radiography [19] and a recent study describes two characteristic appearances on CT: either a localized ground glass opacity which grows slowly (doubling time >1 yr) or a solid mass which grows more rapidly (doubling time <1 yr) [20].

Bronchoalveolar carcinoma

This is regarded as a subtype of adenocarcinoma and represents 2–10% of all primary lung cancers. There are three characteristic presentations: most common is a single pulmonary nodule or mass in 41%; in 36% there may be multicentric or diffuse disease; finally, in 22% there is a localized area of parenchymal consolidation [21]. Bubble-like areas of low attenuation within the mass (fig. 1) are a characteristic finding on CT [22]. Hilar and mediastinal lymphadenopathy is uncommon [23]. Persistent peripheral consolidation with associated nodules in the same lobe or in other lobes should raise the possibility of bronchoalveolar carcinoma [24].

Adenosquamous carcinoma

Adenosquamous carcinoma represents 2% of all lung cancers [16]. This cell type is typically identified as a solitary, peripheral nodule. Over one-half are 1–3 cm in size and cavitation is seen in 13%. Evidence of parenchymal scars or fibrosis in or next to the tumour is seen in 50% [25].

Squamous cell carcinoma

Squamous cell carcinoma represents 30% of all lung cancers [16]. These tumours are more often centrally located within the lung and may grow much larger than 4 cm in diameter [17]. Cavitation (fig. 2) is seen in up to 82% [18]. They commonly cause segmental or lobar lung collapse due to their central location and relative frequency [26].

Small cell lung cancer

Small cell lung cancer (SCLC) represents 18% of all lung cancers [16]. SCLC often present with bulky hila and mediastinal lymph node masses (fig. 3) [27, 28]. A noncontiguous parenchymal mass can be identified in up to 41% at CT [28] that very rarely cavitates [18]. They form the malignant end of a spectrum of neuroendocrine lung carcinomas with typical carcinoid tumours being at the more benign end [27]. A mass in or adjacent to the hilum is characteristic of SCLC and the tumour may well show mediastinal invasion [17].

Carcinoid tumour

Carcinoid tumour represents 1% of all lung cancers [16]. Atypical carcinoid tumours tend to be larger (typically >2.5 cm at CT) with typical carcinoid tumours being more often associated with endobronchial growth (fig. 4) and obstructive pneumonia [27]. Carcinoids tend to be centrally rather than

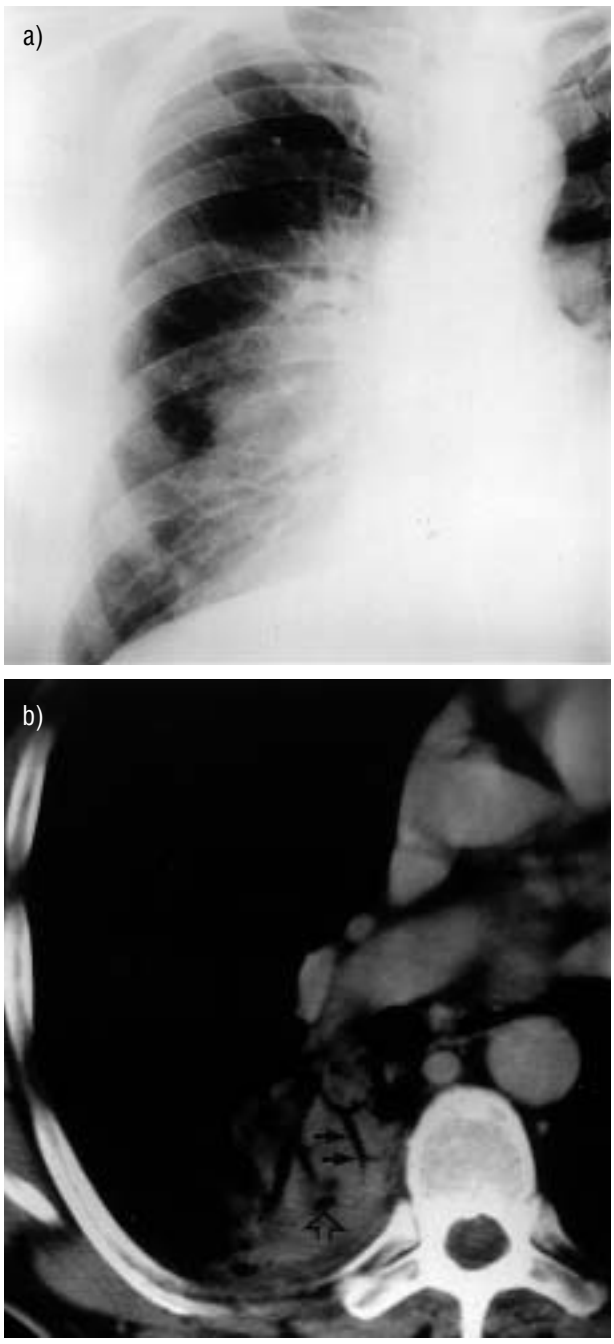

Fig. 1. – a) Diffuse alveolar shadowing in the right lower lobe of a 58-yr-old male presenting as an unresolving pneumonia. b) Air bronchograms (black arrows) and low attenuation lucencies (open arrow) in apical "consolidation", later confirmed as bronchoalveolar carcinoma.

peripherally located and calcification is seen in 26–33% [29]. The 5-yr survival for typical carcinoids is 95% against 57–66% for atypical carcinoids [29].

Large cell carcinoma

Large cell carcinoma represents 9% of all lung cancers [16]. Large or giant cell carcinoma is a poorly differentiated nonsmall cell carcinoma (NSCLC) and

Fig. 2. – A 50-yr-old female with irregular cavitating squamous cell carcinoma in the right upper lobe (arrows).

is diagnosed histologically after exclusion of adenocarcinomatous or squamous differentiation [16]. It may grow extremely rapidly [30] to a large size but metastasizes early to the mediastinum and brain [31].

It should be noted that there seems to be a change occurring in the prevalence of the described histological subtypes. Two large recent trials have reported prevalences for adenocarcinoma of 78% and 58% whilst squamous cell carcinomas accounted for only 4% and 11% respectively [11, 13].

Imaging techniques

Chest radiography

Due to its widespread availability, including to primary care physicians, the chest radiograph is often the first imaging modality to suggest the diagnosis of bronchogenic carcinoma. Lung cancer may present as a straightforward spiculated mass but its presence may also be inferred from other appearances such as an unresolving pneumonia or lobar collapse (fig. 5). In some situations, no further imaging will be necessary when bulky contralateral mediastinal adenopathy is present or when an obvious bony lesion is identified. However, CT scanning of the chest is often needed because of the lack of sensitivity of the chest radiographs in detecting mediastinal lymph node metastases and chest wall and mediastinal invasion [32].

Computed tomography

CT can identify specific features in lung nodules that are diagnostic, *e.g.* arteriovenous fistulae, rounded atelectasis, fungus balls, mucoid impaction and infarcts. High-resolution scanning further refines this

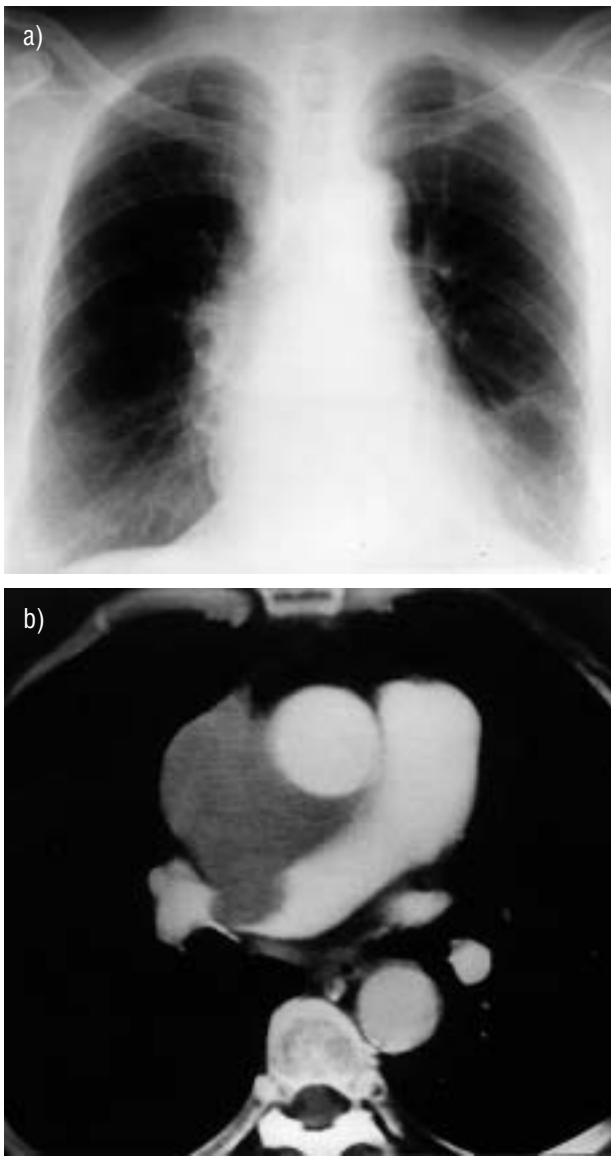

Fig. 3.–a) A 55-yr-old dyspnoeic female. Chest radiograph demonstrating widened mediastinum particularly on the right with reduced vascularity of the right lung. b) Contrast enhanced computed tomography showing central mediastinal mass invading the right pulmonary artery. Small cell carcinoma was confirmed on percutaneous biopsy.

diagnostic process [33]. The ability of CT scanning to evaluate the entire thorax at the time of nodule assessment is of further benefit.

Spiral or helical CT is advantageous as small nodules are not missed between slices as may happen on older, nonspiral machines. It also increases the detection rate of nodules <5 mm in diameter, especially when viewed in cine-format on a workstation [34, 35]. The acquisition of continuous volume data sets permits three-dimensional image reconstruction and multiplanar (*i.e.* nonaxial) reformatting (fig. 6). These techniques have been shown to improve the detection of pleural invasion by tumour and clarify the origin of peridiaphragmatic tumours respectively [36, 37]. Further manipulation of raw

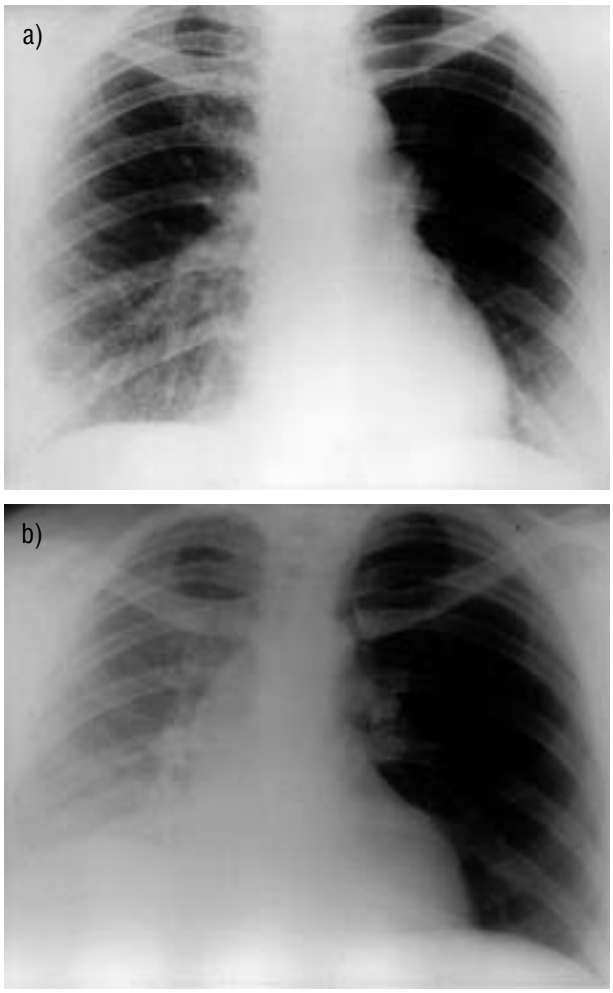

Fig. 4.–a) Inspiratory film with asymmetrical vascularity. b) Expiratory film confirming air trapping due to carcinoid tumour in the left main bronchus.

data sets enables the technique of virtual bronchoscopy. An interactive, simulated bronchoscopy can be performed with the added benefit of simultaneous information on adjacent mediastinal structures. This technique has far reaching potential both as a teaching tool and as a means of evaluating patients′ thoracic and bronchial anatomy prior to interventional procedures and stent placement [38].

The recent advent of multislice scanners has seen advances in image resolution with a substantial reduction in both tube loading and scanning time as up to four slices can be acquired simultaneously [39, 40]. Both spiral and multislice machines suffer less from respiratory motion artefact due to their shorter scanning times.

Spiral CT with a bolus injection of intravenous iodinated contrast medium affords "dynamic scanning". A recent study of 84 patients with NSCLC found no difference in radiological stage when noncontrast enhanced scans were compared with contrast enhanced scans in 80 patients (95%), recommending that nonenhanced CT through the thorax and adrenals was sufficient for staging patients with newly

Fig. 5. – Increased retrocardiac density due to left lower lobe collapse with inferomedial displacement of the hilum.

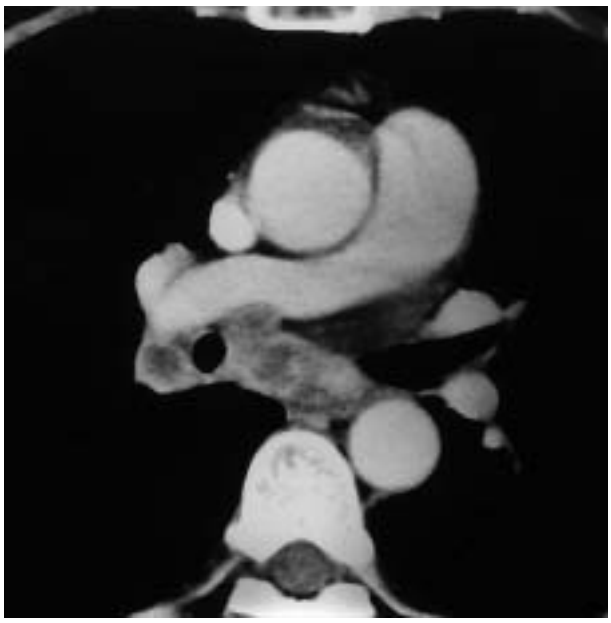

Fig. 7. – Necrotic mediastinal lymph nodes with irregular enhancing rims (arrows).

diagnosed NSCLC [41]. However, another study of 50 patients comparing both techniques found an 11% higher detection rate of enlarged mediastinal nodes after contrast enhancement and recommended its routine administration (figs. 7 and 8) [42]. Many centres perform hepatic and adrenal scans having given intravenous contrast.

Slice thickness and interval should be $\leqslant$10 mm and extend from the lung apices to the adrenal glands [16]. It is now common practice to perform 5-mm slices through the hila and aortopulmonary regions to improve delineation of local lymph nodes and the origins of the lobar bronchi. The field of view should include the contiguous chest wall [16].

Magnetic resonance imaging

Magnetic resonance imaging (MRI) is becoming more available but pressure on MRI scanning time is so intense that it is usually used for problem solving and where administration of contrast media is contraindicated. MRI can be more accurate than CT in separating stage IIIa (resectable) from IIIb (generally unresectable) tumours in selected patients due to its ability to detect invasion of major mediastinal structures, *i.e.* T4 disease [43].

The advantages MRI has over CT include: better soft tissue contrast, multiplanar imaging capability, and therefore useful for superior sulcus tumours and

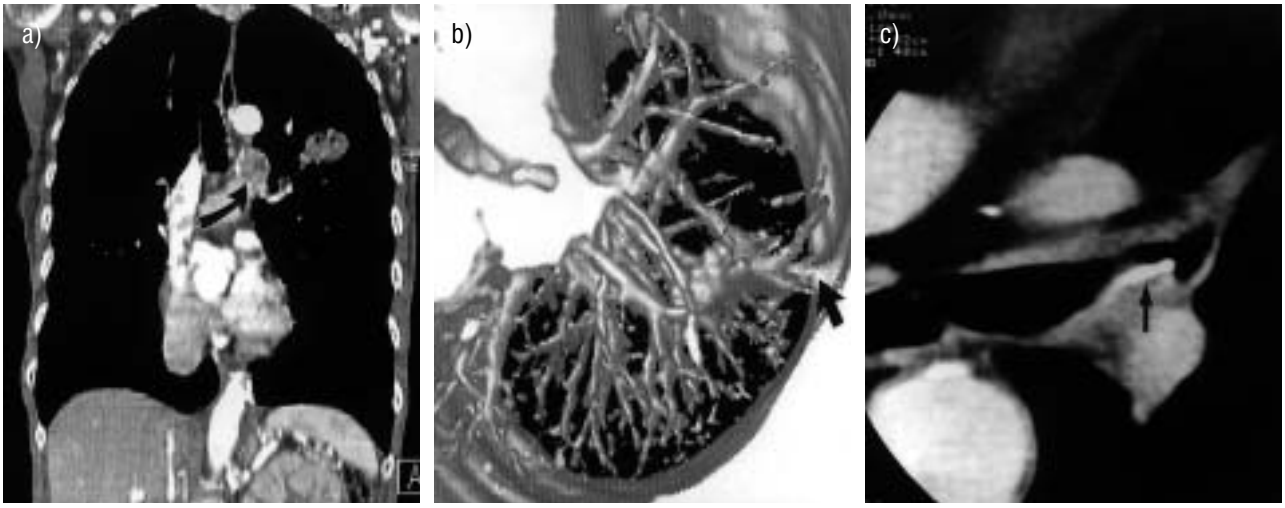

Fig. 6. – a) Coronal reformat from multislice computed tomography (CT) demonstrating mediastinal lymph nodes (arrow) and a necrotic tumour mass within the lung. b) Three-dimensional-reconstruction of a lung tumour with pleural tag (arrow) (images courtesy of T. McArthur, Dept. of Radiology, University College Hospitals, London). c) Thin slice reconstruction in the axial plane from spiral CT data permits the correct identification of an inhaled fish bone (arrow), in a different patient, presumed to be a tumour at bronchoscopy.

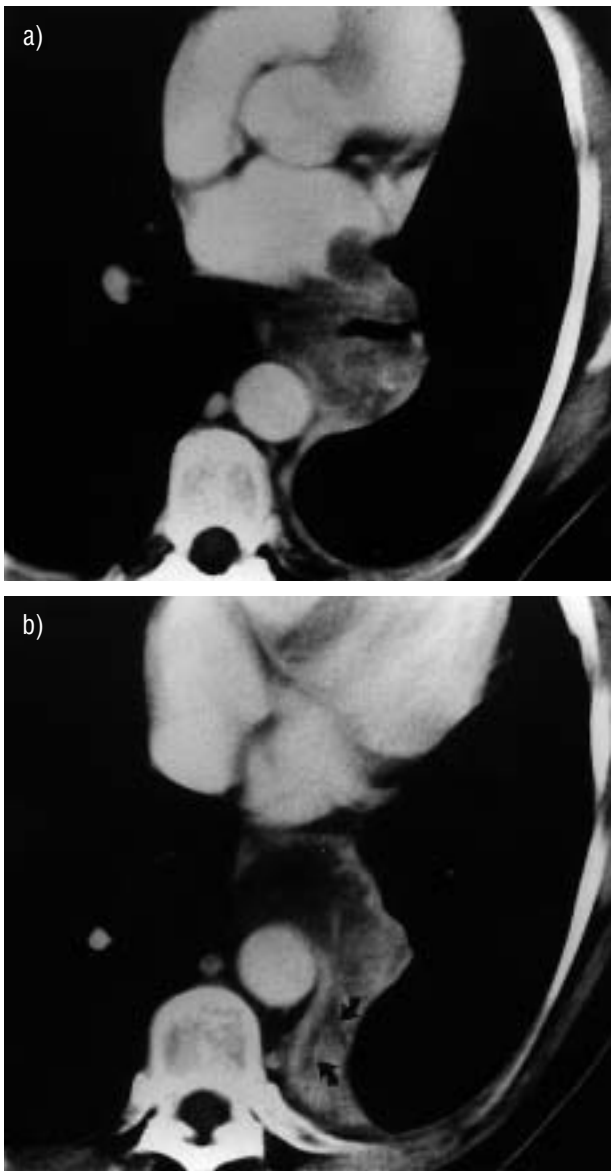

Fig. 8. – a) Mediastinal mass narrowing left lower lobe bronchus and invading left atrium. b) Distal fluid-filled bronchi (arrows) are seen in the collapsed lower lobe due to the proximal tumour.

evaluation of the aortopulmonary window (fig. 9), and cardiac gating which enables excellent delineation of the heart and great vessels and removes cardiac pulsation artefact [44, 45].

MRI is also useful in the assessment of mediastinal and chest wall invasion by virtue of its ability to determine fat-stripe invasion (fig. 10) and involvement of the diaphragm and spinal canal. In addition, it has been shown to aid in differentiating lymph nodes from hila vessels due to the "flow void" phenomenon [46, 47].

MRI has disadvantages compared to CT, being slower and more expensive with poorer spatial resolution and providing limited lung parenchyma information. MRI can overestimate lymph node size because of respiratory movement, causing the blurring together of discrete nodes into a larger, conglomerate mass

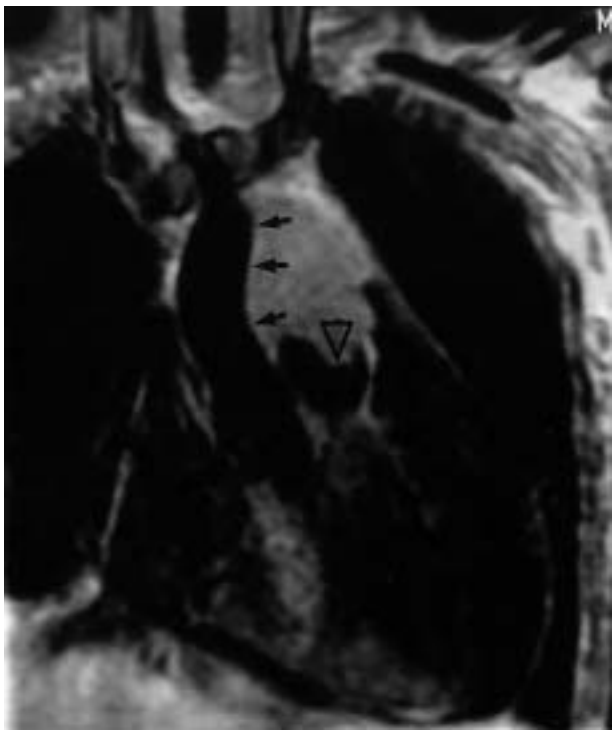

Fig. 9. – Coronal magnetic resonance imaging showing an adenocarcinoma in a young male infiltrating the aortopulmonary window. There is loss of the fat plane against the aorta (arrows) and invasion of the main pulmonary artery (arrowhead).

[44]. MRI is also poorly tolerated by claustrophobic patients and is contra-indicated in patients with indwelling electromagnetic devices and some prosthetic heart valves.

T1-weighted sequences are used for the visualization of fat planes and improved spatial resolution. T2-weighted sequences are useful for detection of high-signal tumour infiltration. Gadolinium enhancement can further enhance the diagnostic yield [48].

Positron emission tomography

Positron emission tomography (PET) scanning is a new imaging modality whose role in the assessment of lung cancer is still being determined. Its advantage over other modalities lies in its sensitivity in detecting malignancy and its ability to image the entire body in one examination.

PET is a physiological imaging technique that uses radiopharmaceuticals produced by labelling metabolic markers such as amino acids or glucose with positron-emitting radio nuclides such as fluorine-18. The radiomarker is then imaged by coincidence detection of two 511 KeV photons that are produced by annihilation of the emitted positrons. The radiopharmaceutical, ^{18}F-2-deoxy-D-glucose (FDG) is ideally suited for tumour imaging. PET performed with this agent exploits the differences in glucose metabolism between normal and neoplastic cells, allowing accurate, non-invasive differentiation of benign *versus* malignant

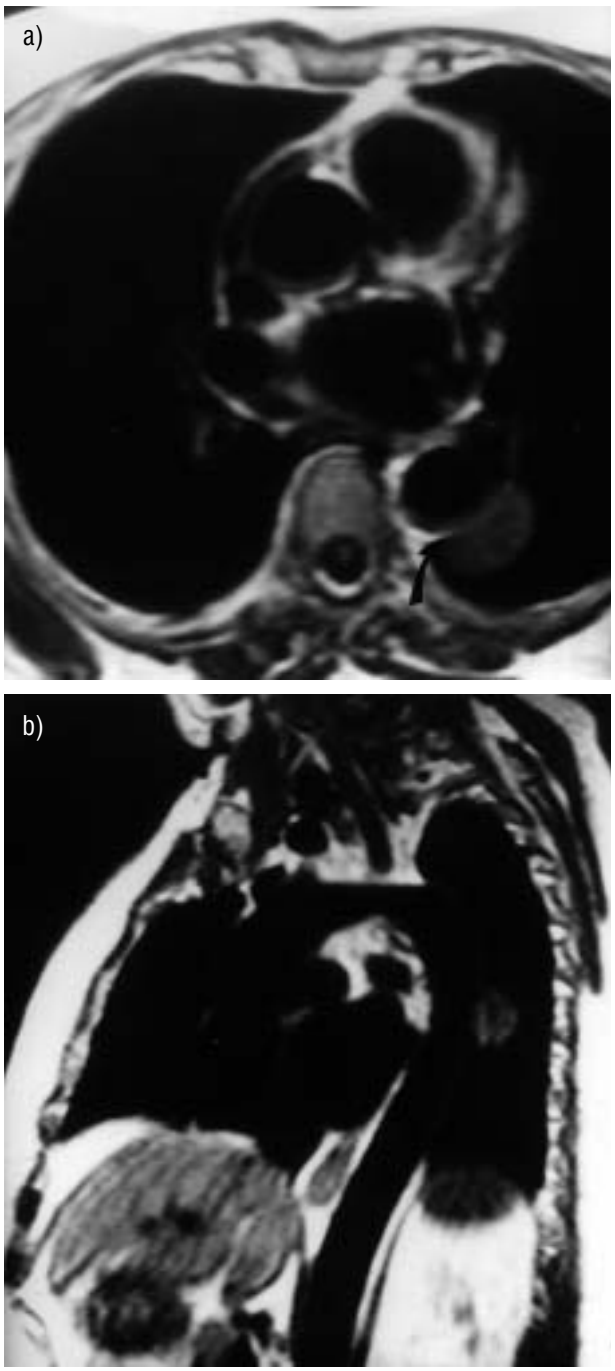

Fig. 10. – T1-weighted images demonstrating superior ability of magnetic resonance imaging in demonstrating loss of fat plane (arrow) in a) axial and b) sagittal planes.

abnormalities [49]. Uptake of FDG is known to be proportional to tumour aggressiveness and growth rates [50]. FDG uptake can be assessed visually on PET images (fig. 11) by comparing the activity of the lesion with the background or by semiquantitative analysis using calculated standardized uptake ratios. An uptake ratio of <2.5 is considered indicative of a benign lesion [51, 52].

PET scanning detects malignancy in focal pulmonary opacities with a sensitivity of 96%, specificity of

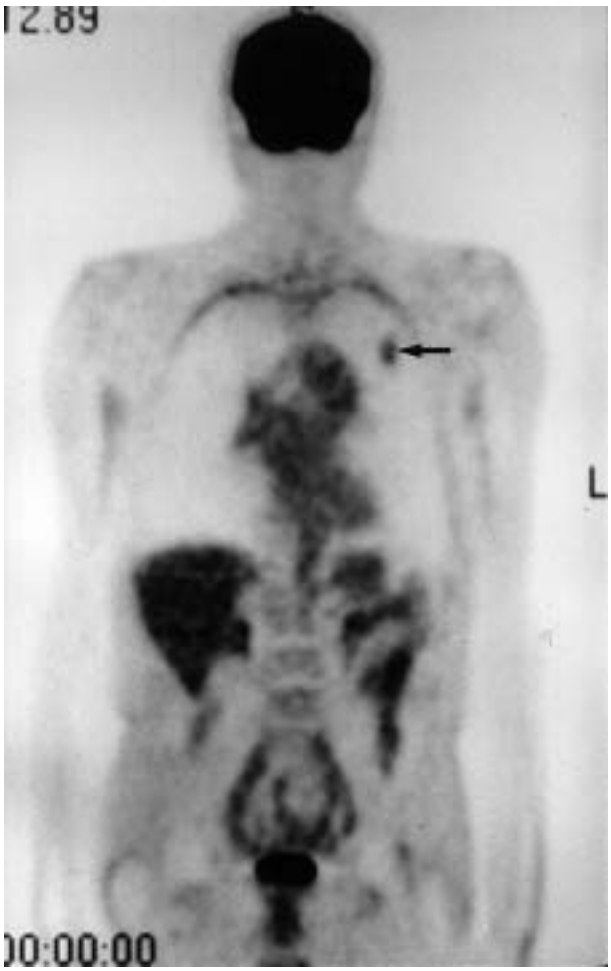

Fig. 11. – Avid uptake of ^{18}F-2-deoxy-D-glucose in left apical tumour (arrow).

88% and an accuracy of 94% in lesions of $\geqslant$10 mm [53–58]. However, compared to CT, PET has poorer spatial resolution, which precludes it from accurate anatomical assessment of primary tumour status [59]. False-positive PET findings in the lung are seen in tuberculous infection, histoplasmosis and rheumatoid lung disease. False negatives are seen with carcinoid tumours, bronchoalveolar carcinoma and lesions <10 mm in size [58–61].

PET is more accurate than CT in the detection or exclusion of mediastinal nodal metastases: sensitivities are 67–100% and 50–63% respectively whilst specificities are 81–100% and 59–94% [62–65]. PET has been shown to correctly increase or decrease nodal staging as initially determined by CT in 21% of presurgical patients [66]. In a study of 50 patients where PET and CT findings were reported jointly, the sensitivity rose to 93%, specificity 97% and accuracy 96% in the detection of mediastinal nodal disease [63]. PET has been shown to detect occult extrathoracic metastases in 11–14% of patients selected for curative resection and alter management in up to 40% of cases [66–68].

In a recent study of 100 patients comparing whole body PET with conventional imaging (thoracic

CT, bone scintigraphy, and brain CT or MRI) in staging bronchogenic carcinoma PET accurately staged NSCLC in 83% of cases when compared with pathological stage [69]. The figure for conventional imaging was 65%. PET identified nine patients with metastases that were missed on conventional imaging whilst 10% of patients suspected of having metastases conventionally, were shown not to have by PET. PET was more sensitive and specific than bone scintigraphy for the detection of bone metastases and had a 100% positive predictive value for the presence of adrenal deposits as against 43% for conventional imaging. The technique faired poorly in the detection of brain metastases (60% sensitivity) prompting the authors to recommend the continued use of conventional imaging for routine staging of the brain. However, the negative predicative value of PET for N3 disease was identical to that of mediastinoscopy (96%) prompting the statement that patients with negative mediastinal PET findings could go directly to surgical resection of the primary lesion [69]. This approach has been supported by other authors [59, 68]. Positive PET findings however warrant nodal biopsy, as guided by the areas of increased FDG uptake, in order to exclude false positives. Causes include infection, inflammation, hyperplasia and sarcoidosis [59].

The main disadvantage for PET is the lack of availability and relatively high cost of each examination. However, decision analysis models indicate that combined use of CT and PET imaging for evaluating focal pulmonary lesions is the most cost-effective and useful strategy in determining patient management with a pretest likelihood of having a malignant nodule of 0.12–0.69 [70].

PET is more accurate than conventional studies in detecting recurrent lung cancer and appears to be superior in distinguishing persistent or recurrent tumour from fibrotic scars [59, 71]. However, false-positive studies do occur secondary to postirradiation inflammatory change and delaying the examination until 4 or 5 weeks postirradiation is recommended [72].

A recent study of 114 patients with solitary pulmonary nodules, $\leqslant$6 cm in diameter, highlighted the usefulness of single photon emission computed tomography using the ^{99m}Technetium-labelled somatostatin analogue, Depreotide [73]. The sensitivity and specificity for this method in determining benign from malignant nodules was 97% and 73% respectively. These results are comparable with FDG-PET imaging and can be performed using a standard gamma camera.

The solitary pulmonary nodule

Only 20% of carcinomas are resectable at diagnosis [74] and 50% of "coin lesions" on chest radiography are malignant: 40% representing primary lung cancers whilst the other 10% are solitary metastases [75]. However, 20–30% of all cancers present as a solitary pulmonary nodule (SPN) of which 88% are resectable with a 5-yr survival rate around 50% [74]. The early identification and correct assessment of such nodules is therefore of the utmost importance.

Benign nodules

Chest radiography. A number of findings enable a nodule to be classed as benign on the basis of chest radiographical findings. 1) Age <35 yrs, no history of cigarette smoking and no history of extrathoracic malignancy [76]. 2) Comparison with old films and establishment of no growth over at least a 2-yr period [32]. 3) If the nodule contains fat density or a benign pattern of calcification such as central nidus-type, popcorn, laminated or diffuse (fig. 12) [33]. Note should be made that eccentric or stippled calcification is seen in ~10% of lung cancers [76]. An appropriate history such as fever or chest pain may promote the likelihood of a benign process such as focal pneumonia or an infarct presenting as an SPN. A repeat radiograph should be performed at 2–6 weeks to assess resolution [76].

Computed tomography scanning, densitometry and enhancement. CT scanning can further refine the detection of calcification and fat within nodules. A total 22–38% of noncalcified nodules on chest radiographs appear calcified on CT [76]. Using CT densitometry, a "pixel map" of a nodule can be created with Hounsfield Unit (HU) values, >200 being indicative of calcification [77, 78]. Only characteristic patterns of calcification such as central, diffuse, laminar or popcorn are indicative of benignity [33]. The presence of fat (-40–-120 HU) or calcification or a combination of the two has been shown to correctly identify 30 of 47 patients (64%) with hamartomas on 2-mm section CT in one series [79]. However, at least one-third of hamartomas in this series contained neither fat nor calcium leading to an indeterminate assessment.

Fig. 12.–Diffusely calcified, well-defined nodule typical of a hamartoma.

Changes in attenuation after intravenous contrast administration at CT can also be used to distinguish benign from malignant parenchymal nodules. In a recent study of 356 nodules (5–40 mm) containing neither fat nor calcification, enhancement of <15 HU postcontrast administration was strongly predictive of benignity [80]. By retrospectively reducing the cut-off threshold to 10 HU it was possible to increase the technique's sensitivity in excluding malignancy from 98 to 100%.

Malignant nodules

A nodule size >3 cm is associated with malignancy in 93–99% of cases [81]. If the nodule is spiculated (fig. 13) 88–94% will be malignant [82–84] although 11% of malignant nodules do have distinct margins [74]. The presence of calcification in larger (>3 cm) and spiculated nodules should not be viewed as indicative of benignity.

Indeterminate nodules

Small size should not be used as a discriminator for exclusion of malignancy. One in seven nodules <1 cm in size have been shown to be malignant [81] and in a recent study of nodules resected at video-assisted thoracoscopic surgery, 31% of nodules <1 cm in size in patients with no known malignancy were malignant [85]. Cavitation and lobulation are not helpful discriminators in favour of malignancy as granulomas and hamartomas can both have these appearances [74].

Central tumours

Distinct from the SPN, central lung cancers often present radiographically as a hila mass or as collapse and consolidation of lung beyond the tumour with accompanying volume loss. Air bronchograms may be seen at CT [17].

Differentiating central tumours from distal collapse can be difficult but is facilitated by bolus contrast administration followed by prompt CT scanning at the level of abnormality (fig. 14). The lung is appreciably enhanced whilst tumour enhancement is minimal and delayed. The most marked difference between the two is seen from 40 s to 2 min after contrast injection [86].

Differentiating central lung tumours from mediastinal masses can also be problematic. In a study of

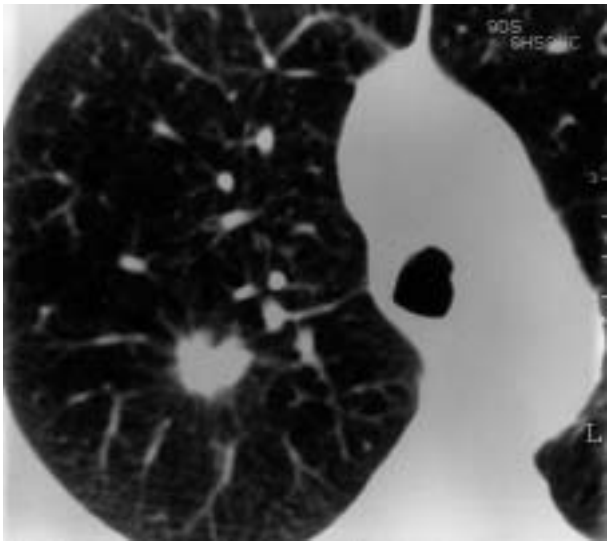

Fig. 13. – Spiculated mass typical of a carcinoma.

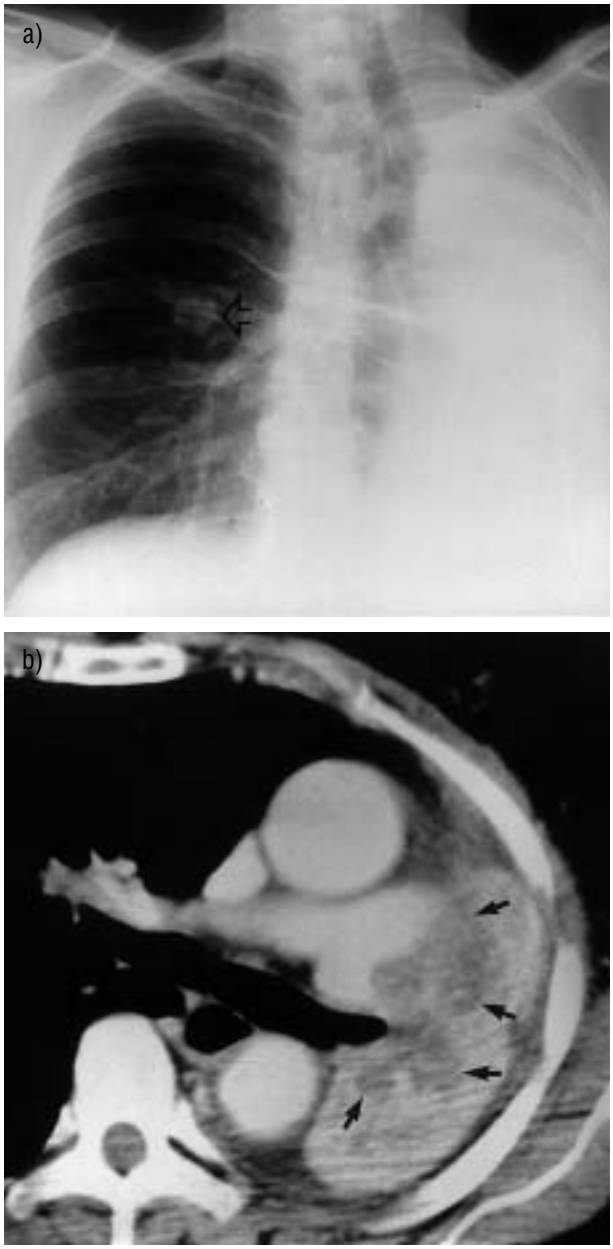

Fig. 14. – a) Collapse of the left lung with mediastinal shift and a right middle zone nodule (arrow). b) Perihilar low attenuation adenocarcinoma (arrows) with distal enhancing collapsed lung in same patient.

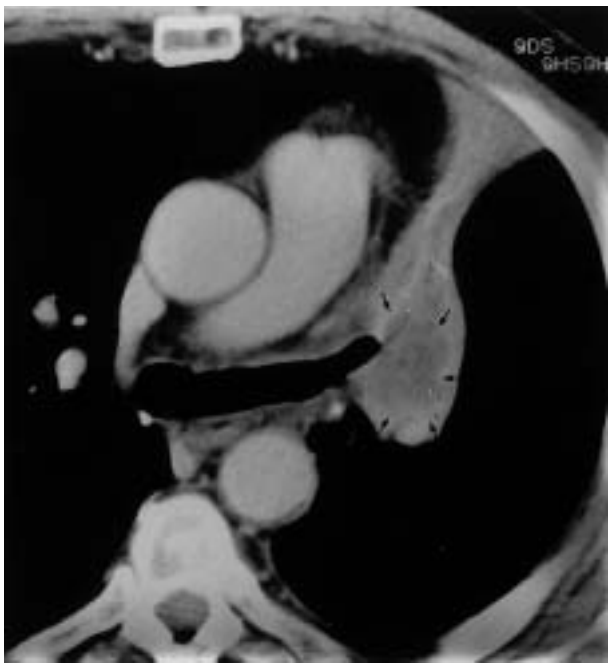

Fig. 15. – Central mass with Golden "S" sign of proximal tumour (arrows) and distal collapse.

90 central lung and mediastinal masses, the single most useful CT finding in distinguishing between the two was the "mass-lung interface". Marginal spiculation, nodularity or irregularity between the mass and the surrounding lung almost always indicated the mass had arisen in the lung. A smooth interface suggested that the mass was mediastinal in location. A notable exception was Hodgkin's lymphoma which may occasionally cross the pleura, invade the lung and result in a poorly marginated mass, mimicking a lung mass [87].

The following features can be viewed as suspicious for an obstructing neoplasm when associated with a pneumonia. 1) The "S" sign of Golden, indicating a fissure deviated around a central tumour mass (fig. 15). 2) Pneumonia confined to one lobe (or more if supplied by a common, obstructed bronchus) especially if >35-yrs-old and accompanied by volume loss or mucus filled bronchi with no air bronchograms present [17]. In an analysis of 50 patients with segmental or lobar atelectasis, 27 (54%) were caused by an obstructing tumour, all of which were detected at CT [88]. 3) Localized pneumonia that persists for >2 weeks or recurs in the same lobe.

Hila enlargement is a common presenting feature in patients with lung cancer [17]. In the Mayo Clinic series, 38% of patients with lung cancer had a hila or peri-hila mass [89]. More recently, 14 of 25 patients (56%) with CT performed for an abnormal hilum were found to have bronchogenic carcinoma [90]. The presence of a tumour mass or enlarged lymph nodes will give a dense hilum. Generally speaking the more lobular the shape the more likely that adenopathy is present [17].

Staging nonsmall cell lung cancer

The revised international system for staging lung cancer [4] incorporates the tumour, node, metastasis (TNM) subset system (tables 2 and 3) and shows improved survival rates with more accurate staging and appropriate selection of patients for definitive surgical treatment by distinguishing the IIIa from the IIIb group (table 4). Percentage survival at 5 yrs by clinical stage for the more advanced stages remains poor, emphasizing the importance of early detection.

The overall UK 5-yr survival of only 5.3% serves to underline the preponderance of advanced-stage disease at presentation [3]. Precise tumour (T) and nodal (N) staging is imperative as it determines subsequent treatment, especially when considering neo-adjuvant therapy for IIIa and IIIb disease. Only approximately

Table 2. – Tumour, node, metastasis (TNM) classification

Tumour	
T1	A tumour ⩽3 cm in greatest dimension, surrounded by lung or visceral pleura, without bronchoscopic evidence of invasion more proximal than the lobar bronchus
T2	A tumour with any of the following features: >3 cm in greatest dimension; involvement of the main bronchus, ⩾2 cm distal to the carina; invasion of the visceral pleura; atelectasis or obstructive pneumonia extending to the hilum but not involving the entire lung
T3	A tumour of any size directly invading any of: chest wall (including superior sulcus tumours), diaphragm, mediastinal pleura or parietal pericardium; or tumour in a main bronchus within 2 cm of the carina but not involving it; or atelectasis of the entire lung
T4	A tumour of any size invading any of: mediastinum, heart, great vessels, trachea, oesophagus, vertebral body or carina; or tumour with a malignant pleural or pericardial effusion or with satellite tumour nodules within the ipsilateral primary-tumour lobe of the lung
Nodes	
N0	No regional lymph node metastases
N1	Metastases to ipsilateral peribronchial and/or hilar nodes and direct tumour extension into intrapulmonary nodes
N2	Metastases to ipsilateral mediastinal and/or subcarinal nodes
N3	Metastases to contralateral mediastinal, contralateral hilar, scalene or supraclavicular nodes
Metastases	
M0	No distant metastases
M1	Distant metastases present

Table 3. – Staging classification

Stage	TNM classification
IA	T1 N0 M0
IB	T2 N0 M0
IIA	T1 N1 M0
IIB	T2 N1 M0
	T3 N0 M0
IIIA	T3 N1 M0
	T1 N2 M0
	T2 N2 M0
	T3 N2 M0
IIIB	T4 N0 M0
	T4 N1 M0
	T4 N2 M0
	T1 N3 M0
	T2 N3 M0
	T3 N3 M0
	T4 N3 M0
IV	Any T Any N M1

TNM: tumour, node, metastasis.

Table 4. – Cumulative percentage survival at 5-yrs post-treatment by clinical stage

Stage	5-yr survival %
Ia	61
Ib	38
IIa	34
IIb	24
IIIa	13
IIIb	5
IV	1

Modified from [4].

one-half of the TNM stages derived from CT agree with operative staging, with patients being both under and over staged [91, 92]. However, quick access to investigation, high histological confirmation rates (at bronchoscopic/transthoracic biopsy or at thoracotomy), routine CT scanning and review of every patient by a thoracic surgeon is known to substantially increase successful surgical resection [93].

Tumour status

The distinction between T3 and T4 tumours is critical because it separates conventional surgical and nonsurgical management [17]. T4 tumours may be readily identified by virtue of their invasion of a vertebral body (fig. 16), obvious invasion of the mediastinum or heart (fig. 17) or the presence of lung parenchymal metastases. T3 tumours can however be more difficult to grade principally because of the difficulties of distinguishing simple extension of the tumour into the mediastinal pleura or pericardium (T3) from actual invasion (T4).

Mediastinal invasion. Minimal invasion of mediastinal fat is considered resectable by many surgeons [94].

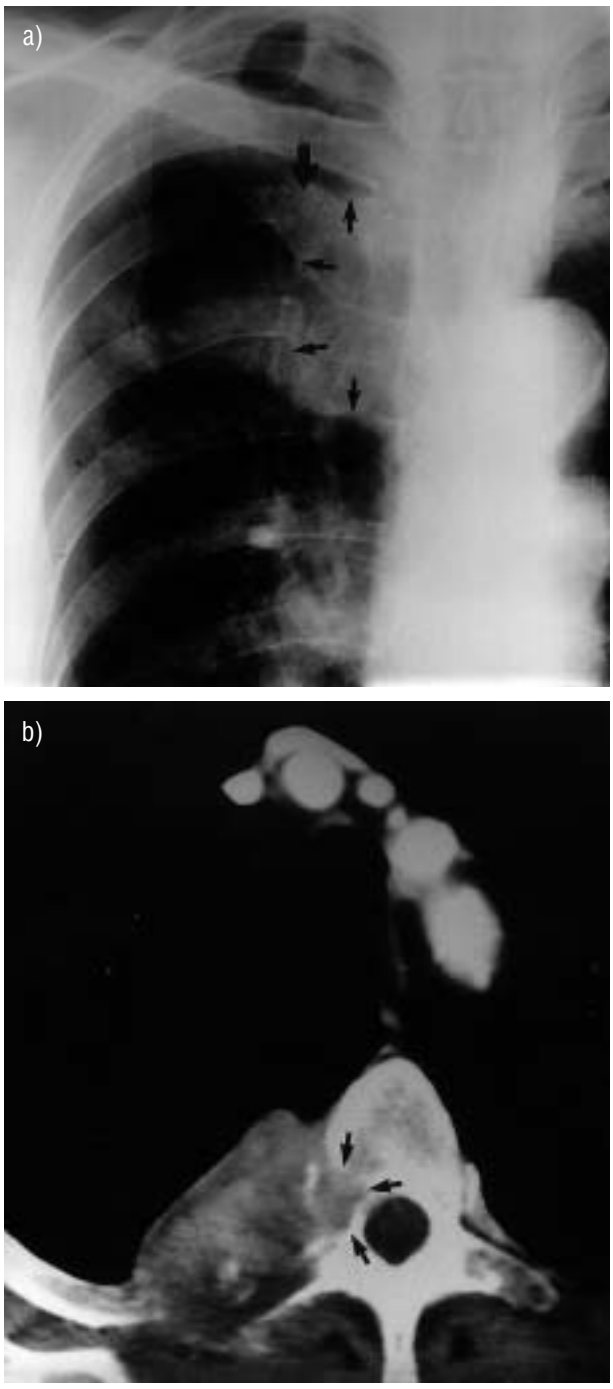

Fig. 16. – a) Rib erosion (large arrow) due to peripheral tumour (small arrows) suggesting at least T3 disease. b) Corresponding computed tomography showing mass eroding rib and vertebral body (arrows) confirming T4 status and inoperability.

Contact with the mediastinum is not enough to diagnose mediastinal invasion [17]. In Glazer's series of 80 CTs considered indeterminate for direct mediastinal invasion, 60% were resectable at thoracotomy with no evidence of mediastinal invasion, 22% did invade the mediastinum but were still technically resectable and only 18% were nonresectable [95]. In fact only one of the 37 masses was not resectable

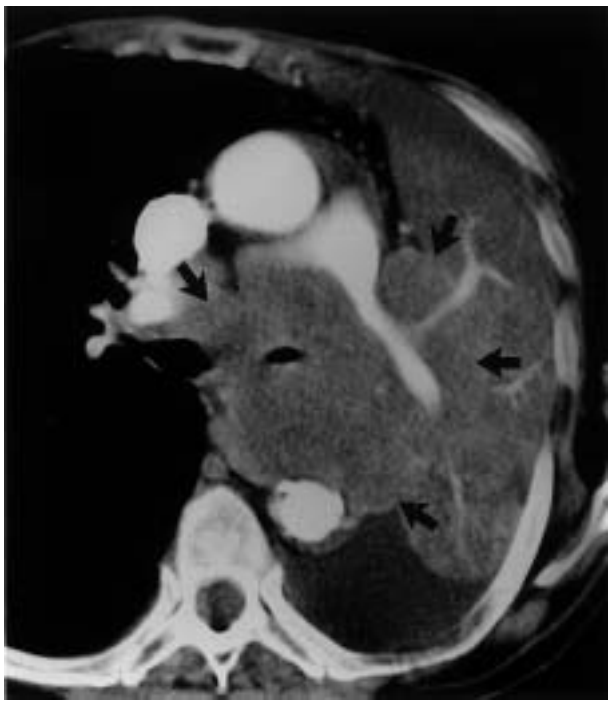

Fig. 17. – Large central mass (arrows) narrowing left main bronchus and encasing left pulmonary artery, indicating T4 status. A pleural effusion is noted.

provided that the pre-operative CT demonstrated at least one of the following: 1) $\leqslant$3 cm contact of the mass with the mediastinum; 2) $<90^{\circ}$ contact with the aorta; 3) fat visible between the mass and mediastinal structures. Importantly however, this information does not identify inoperable tumours (thus avoiding unnecessary thoracotomy) because ~50% of the technically resectable tumours had >3 cm of mediastinal contact or loss of the clear fat plane. Artificial pneumothoraces have been used to improve detection of both mediastinal and chest wall invasion by examining whether or not the pleura peels away from the relevant structure. Although one study demonstrated 100% accuracy for chest wall invasion, its accuracy for mediastinal involvement was only 76% [96]. Another study was 100% sensitive for mediastinal and chest wall invasion but only 80% specific [97]. This again indicated that the technique cannot be categorical about the presence of unresectability.

The Radiologic Diagnostic Oncology Group [98] compared CT and MRI in 170 patients with NSCLC, 90% of whom went on to thoracotomy. There was no significant difference between the sensitivity of the two modalities (63% and 56% respectively) or the specificity (84% and 80%) for distinguishing between T3–4 and T1–2 tumours, except when receiver operating characteristic analysis was performed on the statistics. These showed that MRI is better than CT at diagnosing mediastinal invasion. MRI is particularly useful in determining invasion of the myocardium or tumour extension into the left atrium *via* the pulmonary veins [76].

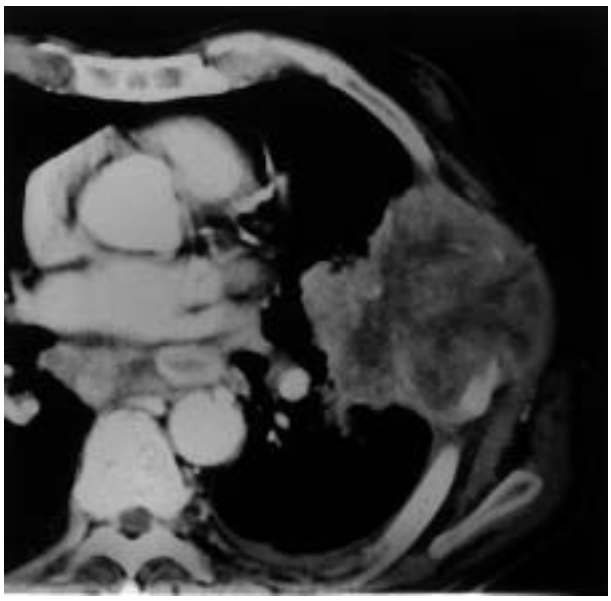

Fig. 18. – Frank chest wall invasion by large peripheral tumour.

Chest wall invasion. CT assessment of tumour chest wall invasion is variable with quoted sensitivities ranging from 38–87% and specificities from 40–90% [94]. Invasion of the chest wall by a mass results in a T3 score. This does not mean the mass is irresectable *per se* but *en bloc* resection of the mass and adjacent chest wall is necessary which carries an associated increase in mortality and morbidity [99]. As well as the technique of inducing artificial pneumothoraces as described earlier, dynamic expiratory multisection CT (viewed as a cine loop) has also been evaluated. In a study of 15 patients, this was found to be 100% accurate for chest wall and mediastinal fixation at pathological examination [100]. With conventional CT imaging, the only reliable criterion for establishing definite invasion is bony destruction with or without tumour mass extending between the ribs and into the chest wall (fig. 18) [94].

Ultrasound has been cited as an additional technique for chest wall assessment (fig. 19). In a series of 120 patients with contiguity between the tumour and the chest wall at CT, 19 patients were judged to have invasive tumour on ultrasound with a sensitivity and specificity of 100% and 98% respectively as compared with operative findings [101].

MRI is a useful technique in establishing chest wall invasion. It relies on the demonstration of infiltration or disruption of the normal extra pleural fat plane on T1-weighted images or parietal pleural signal hyperintensity on T2 weighting. The diagnostic yield is further improved by intravenous gadolinium contrast medium [48]. Sagittal and coronal MRI better display the anatomical relationships at the lung apex as opposed to axial CT (fig. 20). In superior sulcus or Pancoast tumours detection of tumour invasion beyond the lung apex into the brachial plexus, subclavian artery or vertebral body by MRI has been found to be 94% accurate as opposed to 63% for CT [102, 103], although multislice CT with nonaxial reconstruction

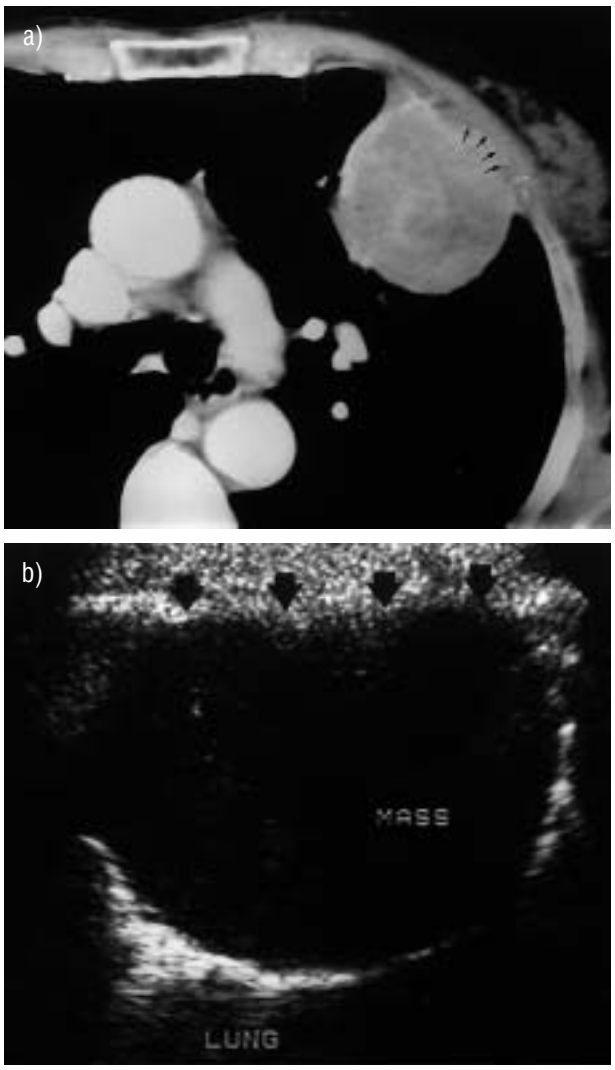

Fig. 19. – a) Computed tomography scan suggesting infiltration of pleural fat (arrows). b) Lack of movement relative to chest wall (arrows) confirms invasion.

may improve this figure. Surface coils and thin sections (5 mm) are advised for MRI of such tumours.

Pleural invasion. Effusions in lung cancer patients can be benign, especially with a postobstructive pneumonia or malignant due to pleural metastases, often characterized by pleural nodularity [94]. Such an effusion renders the tumour T4 and irresectable, though this should be confirmed by thoracocentesis or pleural biopsy.

Nodal status

The most important predictor of outcome in the majority of patients with lung cancer limited to the chest is the presence or absence of involved mediastinal lymph nodes [17]. N3 nodal disease is not an option surgically whilst the management of N2 disease is debatable. Mediastinoscopy and CT are recognized to be the most valuable techniques for evaluation of

Fig. 20. – Coronal T1-weighted magnetic resonance imaging showing subtle Pancoast tumour (open arrow) with extension into the superior sulcus and erosion of the adjacent vertebral body (arrow).

mediastinal lymph node metastases [104] but the arrival of PET has begun to influence patient management in the limited number of centres where it is available.

The enthusiasm for the usefulness of CT in assessing nodal status grew throughout the 1980s. In 1984, LIBSHITZ and MCKENNA [105] demonstrated CT sensitivity and specificity of 67% and 66% respectively using a nodal size of 1 cm to distinguish between benign nodes and those seeded with metastases. In 1988 STAPLES *et al.* [106] demonstrated 79% sensitivity and 65% specificity for CT using a 1-cm long axis nodal cut-off measurement. A meta-analysis in 1990 of 42 CT studies assessing mediastinal lymph node metastases from NSCLC described an overall sensitivity of 0.79, a specificity of 0.78 and an accuracy of 0.79 [107]. However, in 1992 MCLOUD *et al.* [108] using a nodal short axis measurement of 1 cm in 143 patients, returned to less inspiring figures of 64% sensitivity and 62% specificity, respectively. These studies [105, 106, 108] all examined patients with presumed operable lung cancer in whom complete nodal sampling was performed either at mediastinoscopy or thoracotomy. Both LIBSHITZ and MCKENNA [105] and MCLOUD *et al.* [108] observed an increase in false-positive nodes in patients with obstructive pneumonia. MCLOUD *et al.* [103] also found that 37% of nodes, which were 2–3 cm in diameter, did not contain metastases at thoracotomy. More recently in a study of hila and mediastinal nodes at CT compared to pathological examination, sensitivities and specificities for metastatic involvement were only 48% and 53% with an overall accuracy of 51% [92]. Despite these statistics, CT is still recommended as the standard strategy for the investigation of lung cancer

by the Canadian Lung Oncology Group [109] after the study of 685 patients, CT and mediastinoscopy in all patients proving too expensive. They recommended that mediastinoscopy and biopsy be reserved for nodes with a short axis diameter of >1 cm in size (fig. 21). Further refinements of indications for mediastinoscopy have been recommended with its omission in patients with T1 lesions and negative nodes at CT, unless the cell type is adeno- or large cell carcinoma [104]. However, using a CT short axis diameter of 1 cm, SEELY *et al.* [110], whilst examining 104 patients with T1 lesions found nodal metastases at surgery in 21% of cases of which one-third were squamous cell carcinoma.

Others suggest that a negative nodal CT scan does not require mediastinoscopy because even if micrometastases are present, these patients can expect to have better survival if treated surgically than those denied such treatment [76]. Also N2 disease not apparent on CT has been shown to be resectable with up to 30% 5-yr survival [16, 94].

Hila nodes (N1) can usually be resected from hila vessels. Therefore, although pre-operative detection of hila nodes is useful, it is not generally crucial in directing surgical treatment. Moreover, the presence or absence of hila node metastases is an unreliable indicator of mediastinal nodal metastases (N2 disease) [111, 112].

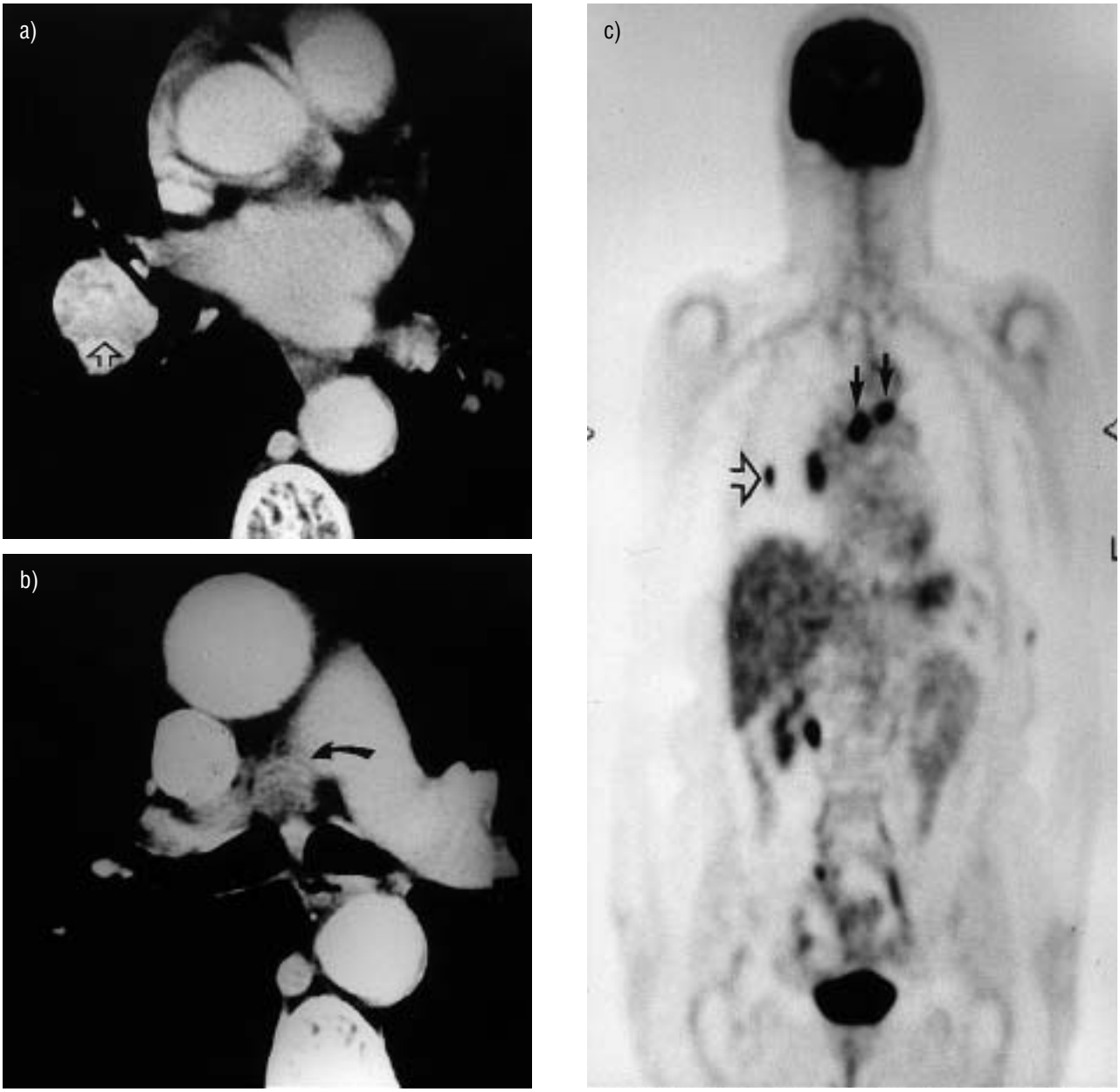

Fig. 21. – Middle-aged-female with a) right hilar mass (arrow) and b) equivocal precarinal lymph node (arrow). c) Positron emission tomography (PET) scan shows increased uptake in mediastinal nodes (arrows) and small peripheral nodule (open arrow). Biopsy of hilar mass confirmed nonsmall cell lung cancer. (PET images courtesy of J. Bomanji, Institute of Nuclear Medicine, University College London).

CT may help to serve as a road map to guide fibreoptic bronchoscopy and biopsy and help identify enlarged nodes that are beyond the reach of the mediastinoscope [16]. It also alerts the surgeon to the presence of anatomical anomalies. No significant difference has been found between the ability of CT and MRI to detect N2 or N3 mediastinal metastases [98]. The combination of respiratory movement artefact and poorer spatial resolution [47] inherent with MRI can mean that small discrete nodes as seen on CT can appear as a larger, indistinct, single nodal mass on MRI, leading to the erroneous diagnosis of nodal enlargement. MRI is also poor at detecting nodal calcification and may thus misclassify enlarged benign nodes as malignant [94].

Metastatic status

A meta-analysis of 25 studies evaluating clinical examination and imaging findings (CT head, abdomen or bone scintigraphy), found the risk of metastases detected by imaging to be <3% if clinical examination is normal [113]. If clinical examination is positive for metastatic disease then metastases will be found by imaging in ~50% of patients. SIDER and HOREJS [114], found extrathoracic metastases in 25% of patients with stage I disease at thoracic CT, brain 11%, bone 8%, liver 6% and adrenals 6% (some patients having more than one site of metastatic spread). Clinically occult metastases were present in only 4% of patients. GRANT *et al.* [115], found distant metastases in patients with no CT evidence of mediastinal disease spread in three of 114 patients (2.5%). Another meta-analysis of 16 studies found that 113 of 2,426 potentially operable patients (4.7%) became inoperable as a consequence of findings at CT scanning of the head and abdomen, ultrasound of the abdomen or scintigraphy of the bone and liver [116].

Liver imaging. QUINT *et al.* [117], found distant metastases in 21% of all NSCLC patients. Relative frequencies were brain 10%, bone 7%, liver 5% and adrenals 3%. Isolated liver metastases were uncommon whilst metastases isolated to the brain were more common leading to the recommendation that CT scanning of the abdomen was not an effective screening method if chest CT is performed.

Imaging of the liver by CT or ultrasound in the absence of clinical signs, symptoms or laboratory abnormalities is controversial and generally not recommended [76]. However, if the adrenals are routinely included on the CT chest scan, as is common practice, then the liver is included by default.

Brain imaging. Two studies have identified 21–64% of brain metastases to be clinically occult prior to CT scanning [118, 119]. KORMAS *et al.* [120], found metastases in 3% of 158 pre-operative patients after negative clinical and laboratory examination. These and other studies [115] recommend CT of the brain routinely in pre-operative patients (fig. 22). More recently however, using a standardized clinical neurological examination as opposed to the KARNOFSKY *et al.* [121] performance scale used in previous studies, COLICE *et al.* [122] found that routine CT of the brain was not indicated with a normal clinical examination. Knowledge of the primary tumour cell type may be helpful in reaching a decision. A recent meta-analysis [113] has found that adenocarcinoma and SCLC are statistically more likely to metastasize to the brain than squamous cell carcinoma. Finally, in a study using contrast enhanced MRI in patients suspected of having surgically resectable NSCLC, localized to the lung or lung and regional nodes, occult brain metastases were identified in 17% of patients with primary tumours >3 cm [123].

Fig. 22. – Computed tomography scan of enhancing cerebral metastasis with marked oedema and mass effect.

Adrenal imaging. In one meta-analysis study up to 7% of patients with carcinoma of the bronchus had adrenal metastases [113]. However, up to 10% of the general population have benign adrenal adenomas [32]. It has been recommended that CT of the adrenals be performed as part of a staging CT of the chest [16]. It involves a minimum amount of extra time, slices and dose to the patient, and is the most cost-effective strategy for evaluating an adrenal mass in a patient with newly diagnosed NSCLC [124]. GILLAMS *et al.* [125] found 4% of 546 patients with lung cancer had solid adrenal tumours. Of these, 23% were proven to be due to malignant infiltration. Benign adenomas tended to be <2 cm in size, of low attenuation, well defined or to involve only part of the gland. Malignant glands tended to be >5 cm and of irregular or mixed

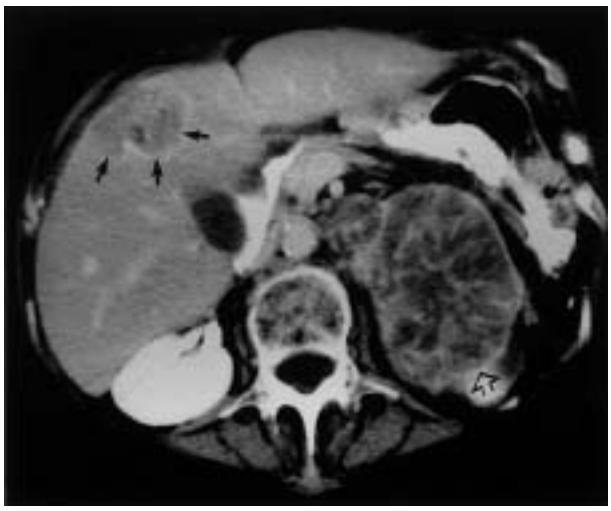

Fig. 23. – Massive left adrenal (open arrow) and hepatic metastases (arrows). M1 disease, stage IV.

attenuation (fig. 23). It was recommended that all indeterminate glands *i.e.* 2–3 cm, undergo fine needle aspiration (FNA) in patients being considered for surgery. This approach is supported elsewhere [16, 32] but it should be noted that MRI can provide additional information *via* chemical or phase shift-imaging regarding the possibility of benignity in such adrenal masses [126, 127]. PET may also have a role to play and has been shown to have a sensitivity of 100% and a specificity of 80% in the detection of metastatic adrenal infiltration in a study of patients presenting with bronchogenic carcinoma and an adrenal mass [128].

Bone imaging. Most bony metastases are symptomatic and bone scintigraphy offers a quick and inexpensive survey of all the bones that is sensitive if not very specific [129]. Alternatively, the presence of a pathological fracture, raised serum alkaline phosphatase and calcium or other nonspecific findings of metastatic disease should similarly prompt a bone scan [16].

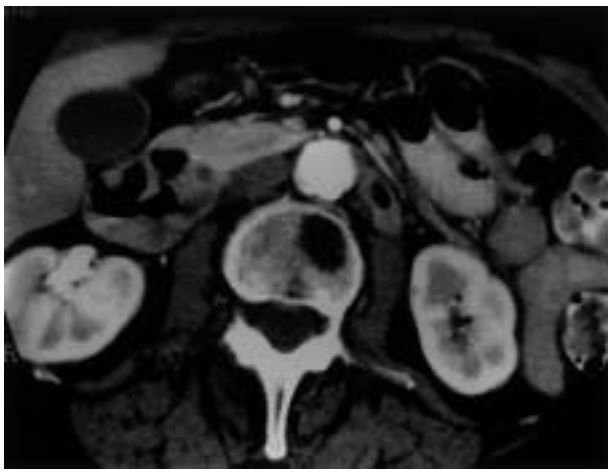

Fig. 24. – Vertebral body metastasis.

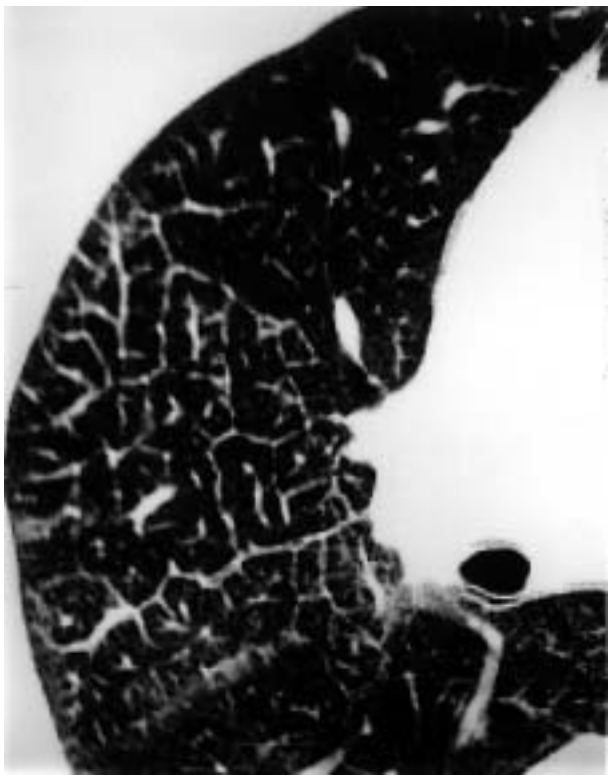

Fig. 25. – Characteristic septal nodular thickening on high-resolution scans typical of lymphangitis carcinomatosa.

Metastases may also be detected on staging thoracic CTs (fig. 24).

Lymphangitis carcinomatosa. Malignant infiltration of the lymphatics and perilymphatic connective tissue is typically asymmetrical and nodular and must be differentiated from left ventricular failure. It is best demonstrated on HRCT scanning (fig. 25).

Staging small cell lung cancer

SCLC is distinguished from NSCLC by its rapid tumour doubling time, development of early widespread metastases and almost exclusive occurrence in smokers [130]. It is divided into two stages: limited disease, which is confined to the ipsilateral hemithorax within a single, tolerable radiotherapy port and extensive disease which covers all other disease including distant metastases. Systemic therapy is required for all patients with SCLC, even those with limited disease. Mediastinal radiotherapy is not always indicated in patients with extensive disease making the distinction between the two stages important. To avoid an exhaustive search for extensive disease (*e.g.* chest, liver, adrenal and cranial CT, bone scans, marrow aspirates *etc.*) an alternative approach is to allow clinical symptoms to direct imaging, terminating on the discovery of extensive disease [130]. Given the fact that cranial CT in SCLC is positive in ~15% of patients at diagnosis, one-third of whom are asymptomatic and that early treatment

of brain metastases yields a lower rate of chronic neurological morbidity, it seems reasonable to begin any extrathoracic staging with brain imaging [32, 130].

Image guided needle biopsy

Transthoracic needle biopsy of a primary lung tumour is controversial when considering a solitary nodule or mass. A negative biopsy needs repeating and the patient will invariably proceed to surgery unless a positive benign result is obtained. Biopsy is useful in determining cell type in inoperable disease to guide further therapy and is essential to confirm the presence of distant metastatic disease.

Needle biopsy is usually performed under either ultrasound or CT guidance. Ultrasound guided biopsy is quick and allows the operator to guide the needle under direct vision but can only be used with peripheral tumours that abut the pleura or invade the chest wall. It is then usually possible to obtain a tissue core using an 18-gauge cutting needle although FNA may be used. CT guided biopsy takes longer and systemic analgesia and sedation may be necessary to maintain patient compliance.

CT affords good visualization of all thoracic structures and CT guided biopsy has an accuracy for diagnosing malignancy of 80–95% [131, 132]. It is the procedure of choice for sampling peripheral nodules (<2 cm in diameter) as the yield for transbronchial needle biopsy, in the absence of an endobronchial lesion, falls from 92–95% to 50–80% [132]. FNA is the preferred sampling method of parenchymal nodules in order to reduce the incidence of complications and is known to have a similar sensitivity in detecting malignancy as core biopsy [131]. However, small tissue fragments for histological evaluation can generally be obtained with 19–22 gauge needles in 40–75% of patients [132]. Such evaluation is valuable because it lends confidence to a cytological diagnosis of cancer, to cell-type determination and to the reliability of a negative result [131, 132]. When a cavitatory or necrotic lesion is encountered, sampling of the wall is recommended to obtain viable tumour material. A single negative biopsy does not exclude malignancy and should prompt a repeat biopsy.

When performing biopsies of mediastinal lesions it is usually possible to use an 18-gauge cutting needle after selecting a safe route. This is especially important in the diagnosis of lymphomas. Cutting needles are also employed in the biopsy of presumed hepatic and adrenal metastases although FNA of the latter may be necessary with smaller lesions (figs. 26 and 27).

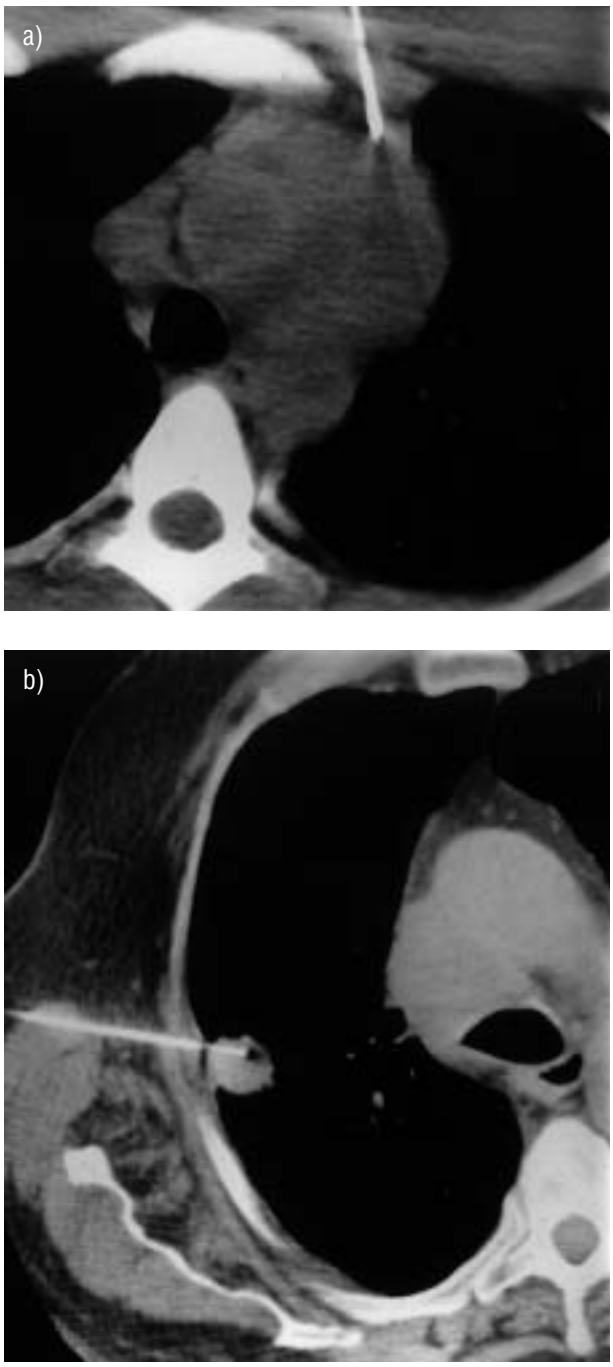

Fig. 26. – Versatility of transthoracic needle biopsy with needle tip in a) mediastinal mass (note safe approach) and b) peripheral solitary nodule.

Conclusion

Lung cancer is a common disease that has a poor prognosis. Survival is inversely proportional to the stage, with early detection and diagnosis being the key to achieving surgical cure. Cross-sectional imaging is now the main radiological means of assessment. Chest radiography is still important, and frequently suggests the first diagnosis, but its relative insensitivity has led to CT scanning being currently evaluated in screening studies.

Currently there is little to choose between CT and MRI in staging the disease although CT is more widely available and less expensive. PET imaging offers heightened sensitivity for both detection of the primary malignancy and disease spread, although it is not 100% accurate and is only available in a few centres. CT scanners are becoming more sophisticated

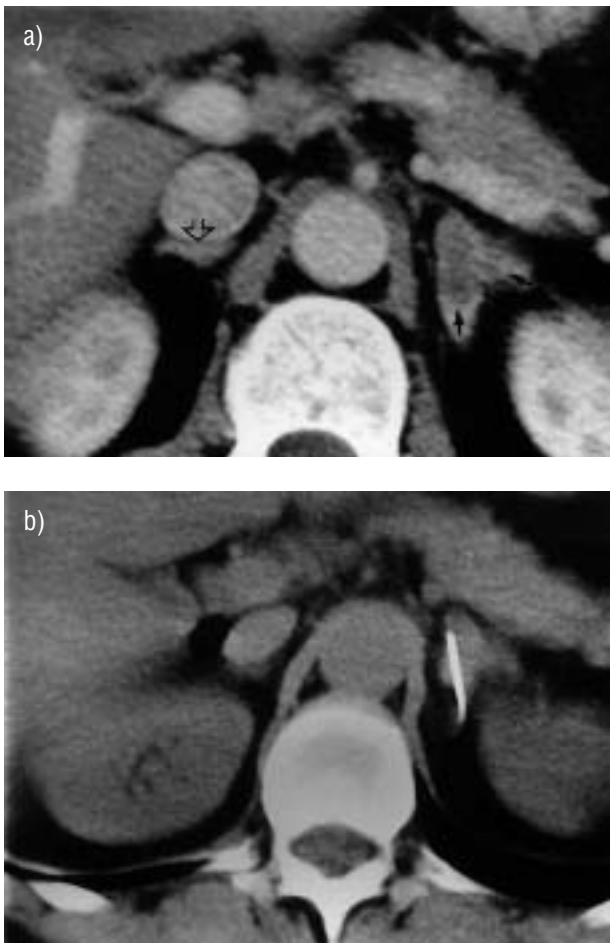

Fig. 27. – a) Low attenuation adrenal mass (arrows) with normal right adrenal (open arrow) which at biopsy, b) confirmed metastatic deposits.

in design and versatility and seem likely to remain the principal imaging modality for this disease in the near future.

References

1. Landis SH, Murray T, Bolden S, Wingo PA. Cancer statistics. *Ca: a Cancer Journal for Clinicians* 1998; 48: 6–29.
2. Patz EF Jr, Goodman PC, Bepler G. Screening for lung cancer. *N Engl J Med* 2000; 343: 1627–1633.
3. Richards MA, Stockton D, Babb P, Coleman MP. How many deaths have been avoided through improvements in cancer survival? *BMJ* 2000; 320: 895–898.
4. Mountain CF. Revisions in the International System for Staging Lung Cancer. *Chest* 1997; 111: 1710–1717.
5. Smith IE. Screening for lung cancer: time to think positive. *Lancet* 1999; 354: 86–87.
6. Tockman M. Survival and mortality from lung cancer in a screening population: the Johns Hopkins study. *Chest* 1986; 89: 324S–326S.
7. Fontana RS, Sanderson DR, Woolner LB, Taylor WF, Miller WE, Muhm JR. Lung cancer screening: the Mayo program. *J Occup Med* 1986; 28: 746–750.
8. Frost JK, Ball WC Jr, Levin ML, *et al.* Early lung cancer detection: results of the initial (prevalence) radiologic and cytologic screening in the Johns Hopkins study. *Amer Rev Respir Dis* 1984; 130: 549–554.
9. Melamed MR, Flehinger BJ, Zaman MB, Heelan RT, Perchick WA, Martini N. Screening for early lung cancer. Results of the Memorial Sloan-Kettering study in New York. *Chest* 1984; 86: 44–53.
10. Kubik A, Parkin DM, Khlat M, Erban J, Polak J, Adamec M. Lack of benefit from semi-annual screening for cancer of the lung: follow-up report of a randomized controlled trial on a population of high-risk males in Czechoslovakia. *Int J Cancer* 1990; 45: 26–33.
11. Henschke CI, McCauley DI, Yankelevitz DF, *et al.* Early Lung Cancer Action Project: overall design and findings from baseline screening. *Lancet* 1999; 354: 99–105.
12. Kaneko M, Eguchi K, Ohmatsu H, *et al.* Peripheral lung cancer: screening and detection with low-dose spiral CT *versus* radiography. *Radiology* 1996; 201: 798–802.
13. Sone S, Takashima S, Li F, *et al.* Mass screening for lung cancer with mobile spiral computed tomography scanner. *Lancet* 1998; 351: 1242–1245.
14. Wan H, Karesen R, Hervik A, Thoresen SO. Mammography screening in Norway: results from the first screening round in four counties and cost-effectiveness of a modeled nationwide screening. *Cancer Causes Control* 2001; 12: 39–45.
15. Sone S, Li F, Yang ZG, *et al.* Results of three-year mass screening programme for lung cancer using mobile low-dose spiral computed tomography scanner. *Br J Cancer* 2001; 84: 25–32.
16. Pretreatment evaluation of non-small-cell lung cancer. The American Thoracic Society and The European Respiratory Society. *Amer J Respir Crit Care Med* 1997; 156: 320–332.
17. Armstrong P. Neoplasms of the lungs, airways and pleura. *In*: Armstrong P, Wilson AG, Dee P, Hansell DM, eds. Imaging of Diseases of the Chest. 3rd edition. London, Mosby (Harcourt), 2000; pp. 305–401.
18. Chaudhuri MR. Primary pulmonary cavitating carcinomas. *Thorax* 1973; 28: 354–366.
19. Woodring JH, Stelling CB. Adenocarcinoma of the lung: a tumor with a changing pleomorphic character. *Am J Roentgenol* 1983; 140: 657–664.
20. Aoki T, Nakata H, Watanabe H, *et al.* Evolution of peripheral lung adenocarcinomas: CT findings correlated with histology and tumor doubling time. *Am J Roentgenol* 2000; 174: 763–768.
21. Bonomo L, Storto ML, Ciccotosto C, *et al.* Bronchioloalveolar carcinoma of the lung. *Eur Radiol* 1998; 8: 996–1001.
22. Zwirewich CV, Vedal S, Miller RR, Muller NL. Solitary pulmonary nodule: high-resolution CT and radiologic-pathologic correlation. *Radiology* 1991; 179: 469–476.
23. Clark LR, Stull MA, Twigg HL. Chest case of the day. Bronchoalveolar carcinoma of the lung. *Am J Roentgenol* 1990; 154: 1318–1319.
24. Aquino SL, Chiles C, Halford P. Distinction of consolidative bronchioloalveolar carcinoma from pneumonia: do CT criteria work? *Am J Roentgenol* 1998; 171: 359–363.
25. Kazerooni EA, Bhalla M, Shepard JA, McLoud TC.

Adenosquamous carcinoma of the lung: radiologic appearance. *Am J Roentgenol* 1994; 163: 301–306.
26. Byrd RB, Miller WE, Carr DT, Payne WS, Woolner LB. The roentgenographic appearance of squamous cell carcinoma of the bronchus. *Mayo Clinic Proceedings* 1968; 43: 327–332.
27. Forster BB, Muller NL, Miller RR, Nelems B, Evans KG. Neuroendocrine carcinomas of the lung: clinical, radiologic, and pathologic correlation. *Radiology* 1989; 170: 441–445.
28. Pearlberg JL, Sandler MA, Lewis JW Jr, Beute GH, Alpern MB. Small-cell bronchogenic carcinoma: CT evaluation. *Am J Roentgenol* 1988; 150: 265–268.
29. Dahnert W. Chest Disorders. *In*: Dahnert W, ed. Radiology Review Manual. 3rd edition. Baltimore, Williams and Wilkins, 1996; pp. 346–346.
30. Fraser RG, Parre JAP. Diagnosis of diseases of the chest. 4th edition. Philadelphia, W.B. Saunders, 1999; pp. 1142–1143.
31. Shin MS, Jackson LK, Shelton RW Jr, Greene RE. Giant cell carcinoma of the lung. Clinical and roentgenographic manifestations. *Chest* 1986; 89: 366–369.
32. Hyer JD, Silvestri G. Diagnosis and staging of lung cancer. *Clin Chest Med* 2000; 21: 95–106.
33. Webb WR. Radiologic evaluation of the solitary pulmonary nodule. *Am J Roentgenol* 1990; 154: 701–708.
34. Remy-Jardin M, Remy J, Giraud F, Marquette CH. Pulmonary nodules: detection with thick-section spiral CT *versus* conventional CT. *Radiology* 1993; 187: 513–520.
35. Tillich M, Kammerhuber F, Reittner P, Riepl T, Stoeffler G, Szolar DH. Detection of pulmonary nodules with helical CT: comparison of cine and film-based viewing. *Am J Roentgenol* 1997; 169: 1611–1614.
36. Brink JA, Heiken JP, Semenkovich J, Teefey SA, McClennan BL, Sagel SS. Abnormalities of the diaphragm and adjacent structures: findings on multiplanar spiral CT scans. *Am J Roentgenol* 1994; 163: 307–310.
37. Kuriyama K, Tateishi R, Kumatani T, *et al.* Pleural invasion by peripheral bronchogenic carcinoma: assessment with three-dimensional helical CT. *Radiology* 1994; 191: 365–369.
38. Aquino SL, Vining DJ. Virtual bronchoscopy. *Clin Chest Med* 1999; 20: 725–730.
39. Ohnesorge B, Flohr T, Schaller S, *et al.* The technical bases and uses of multi-slice CT. *Radiologe* 1999; 39: 923–931.
40. McCollough CH, Zink FE. Performance evaluation of a multi-slice CT system. *Med Phys* 1999; 26: 2223–2230.
41. Patz EF Jr, Erasmus JJ, McAdams HP, *et al.* Lung cancer staging and management: comparison of contrast-enhanced and nonenhanced helical CT of the thorax. *Radiology* 1999; 212: 56–60.
42. Cascade PN, Gross BH, Kazerooni EA, *et al.* Variability in the detection of enlarged mediastinal lymph nodes in staging lung cancer: a comparison of contrast-enhanced and unenhanced CT. *Am J Roentgenol* 1998; 170: 927–931.
43. Gefter WB. Magnetic resonance imaging in the evaluation of lung cancer. *Semin Roentgen* 1990; 25: 73–84.
44. Hatabu H, Stock KW, Sher S, *et al.* Magnetic resonance imaging of the thorax. Past, present, and future. *Clin Chest Med* 1999; 20: 775–803.
45. Batra P, Brown K, Steckel RJ, Collins JD, Ovenfors CO, Aberle D. MR imaging of the thorax: a comparison of axial, coronal, and sagittal imaging planes. *J Comp Assist Tomogr* 1988; 12: 75–81.
46. Aitken K, Armstrong P. Clinical imaging for staging lung cancer. *Imaging* 1992; 4: 15–22.
47. Webb WR, Jensen BG, Sollitto R, *et al.* Bronchogenic carcinoma: staging with MR compared with staging with CT and surgery. *Radiology* 1985; 156: 117–124.
48. Padovani B, Mouroux J, Seksik L, *et al.* Chest wall invasion by bronchogenic carcinoma: evaluation with MR imaging. *Radiology* 1993; 187: 33–38.
49. Erasmus JJ, Patz EF Jr. Positron emission tomography imaging in the thorax. *Clin Chest Med* 1999; 20: 715–724.
50. Duhaylongsod FG, Lowe VJ, Patz EF Jr, Vaughn AL, Coleman RE, Wolfe WG. Lung tumor growth correlates with glucose metabolism measured by fluoride-18 fluorodeoxyglucose positron emission tomography. *Annals of Thoracic Surgery* 1995; 60: 1348–1352.
51. Lowe VJ, Fletcher JW, Gobar L, *et al.* Prospective investigation of positron emission tomography in lung nodules. *J Clin Oncol* 1998; 16: 1075–1084.
52. Lowe VJ, Duhaylongsod FG, Patz EF, *et al.* Pulmonary abnormalities and PET data analysis: a retrospective study. *Radiology* 1997; 202: 435–439.
53. Conti PS, Lilien DL, Hawley K, Keppler J, Grafton ST, Bading JR. PET and [18F]-FDG in oncology: a clinical update. *Nucl Med Biol* 1996; 23: 717–735.
54. Gupta NC, Frank AR, Dewan NA, *et al.* Solitary pulmonary nodules: detection of malignancy with PET with 2-[F-18]-fluoro-2-deoxy-D-glucose. *Radiology* 1992; 184: 441–444.
55. Gupta NC, Maloof J, Gunel E. Probability of malignancy in solitary pulmonary nodules using fluorine-18-FDG and PET. *J Nucl Med* 1996; 37: 943–948.
56. Hubner KF, Buonocore E, Gould HR, *et al.* Differentiating benign from malignant lung lesions using "quantitative" parameters of FDG PET images. *Clin Nucl Med* 1996; 21: 941–949.
57. Patz EF Jr, Lowe VJ, Hoffman JM, *et al.* Focal pulmonary abnormalities: evaluation with F-18 fluorodeoxyglucose PET scanning. *Radiology* 1993; 188: 487–490.
58. Scott WJ, Schwabe JL, Gupta NC, Dewan NA, Reeb SD, Sugimoto JT. Positron emission tomography of lung tumors and mediastinal lymph nodes using [18F]fluorodeoxyglucose. The Members of the PET-Lung Tumor Study Group. *Annals of Thoracic Surgery* 1994; 58: 698–703.
59. Erasmus JJ, McAdams HP, Patz EF Jr. Non-small cell lung cancer: FDG-PET imaging. *J Thorac Imaging* 1999; 14: 247–256.
60. Erasmus JJ, McAdams HP, Patz EF Jr, Coleman RE, Ahuja V, Goodman PC. Evaluation of primary pulmonary carcinoid tumors using FDG PET. *Am J Roentgenol* 1998; 170: 1369–1373.
61. Jang HJ, Lee KS, Kwon OJ, Rhee CH, Shim YM, Han J. Bronchioloalveolar carcinoma: focal area of ground-glass attenuation at thin-section CT as an early sign. *Radiology* 1996; 199: 485–488.
62. Steinert HC, Hauser M, Allemann F, *et al.* Non-small cell lung cancer: nodal staging with FDG PET *versus* CT with correlative lymph node mapping and sampling. *Radiology* 1997; 202: 441–446.

63. Vansteenkiste JF, Stroobants SG, De Leyn PR, *et al.* Mediastinal lymph node staging with FDG-PET scan in patients with potentially operable non-small cell lung cancer: a prospective analysis of 50 cases. Leuven Lung Cancer Group. *Chest* 1997; 112: 1480–1486.
64. Guhlmann A, Storck M, Kotzerke J, Moog F, Sunder-Plassmann L, Reske SN. Lymph node staging in non-small cell lung cancer: evaluation by [18F]FDG positron emission tomography (PET). *Thorax* 1997; 52: 438–441.
65. Dwamena BA, Sonnad SS, Angobaldo JO, Wahl RL. Metastases from non-small cell lung cancer: mediastinal staging in the 1990s-meta-analytic comparison of PET and CT. *Radiology* 1999; 213: 530–536.
66. Valk PE, Pounds TR, Hopkins DM, *et al.* Staging non-small cell lung cancer by whole-body positron emission tomographic imaging. *Ann Thorac Surg* 1995; 60: 1573–1581.
67. Lewis P, Griffin S, Marsden P, *et al.* Whole-body 18F-fluorodeoxyglucose positron emission tomography in preoperative evaluation of lung cancer. *Lancet* 1994; 344: 1265–1266.
68. Weder W, Schmid RA, Bruchhaus H, Hillinger S, von Schulthess GK, Steinert HC. Detection of extrathoracic metastases by positron emission tomography in lung cancer. *Ann Thorac Surg* 1998; 66: 886–892.
69. Marom EM, McAdams HP, Erasmus JJ, *et al.* Staging non-small cell lung cancer with whole-body PET. *Radiology* 1999; 212: 803–809.
70. Gambhir SS, Shepherd JE, Shah BD, *et al.* Analytical decision model for the cost-effective management of solitary pulmonary nodules. *J Clin Oncol* 1998; 16: 2113–2125.
71. Bury T, Corhay JL, Duysinx B, *et al.* Value of FDG-PET in detecting residual or recurrent nonsmall cell lung cancer. *Eur Respir J* 1999; 14: 1376–1380.
72. Frank A, Lefkowitz D, Jaeger S, *et al.* Decision logic for retreatment of asymptomatic lung cancer recurrence based on positron emission tomography findings. *Int J Radiat Oncol Bio Phys* 1995; 32: 1495–1512.
73. Blum J, Handmaker H, Lister-James J, Rinne N. A multicenter trial with a somatostatin analog 99mTc Depreotide in the evaluation of solitary pulmonary nodules. *Chest* 2000; 117: 1232–1238.
74. Viggiano RW, Swensen SJ, Rosenow EC III. Evaluation and management of solitary and multiple pulmonary nodules. *Clin Chest Med* 1992; 13: 83–95.
75. Webb WR. The solitary pulmonary nodule. *In*: Freundlich IM, Bragg DG, eds. A radiologic approach to diseases of the chest. Baltimore, Williams and Williams, 1997; pp. 101–108.
76. McLoud TC, Swenson SJ. Lung carcinoma. *Clin Chest Med* 1999; 20: 697–713.
77. Im JG, Gamsu G, Gordon D, *et al.* CT densitometry of pulmonary nodules in a frozen human thorax. *Am J Roentgenol* 1988; 150: 61–66.
78. Siegelman SS, Khouri NF, Scott WW Jr, *et al.* Pulmonary hamartoma: CT findings. *Radiology* 1986; 160: 313–317.
79. Siegelman SS, Khouri NF, Leo FP, Fishman EK, Braverman RM, Zerhouni EA. Solitary pulmonary nodules: CT assessment. *Radiology* 1986; 160: 307–312.
80. Swensen SJ, Viggiano RW, Midthun DE, *et al.* Lung nodule enhancement at CT: multicenter study. *Radiology* 2000; 214: 73–80.
81. Zerhouni EA, Stitik FP, Siegelman SS, *et al.* CT of the pulmonary nodule: a cooperative study. *Radiology* 1986; 160: 319–327.
82. Westcott JL. Percutaneous transthoracic needle biopsy. *Radiology* 1988; 169: 593–601.
83. Huston J III, Muhm JR. Solitary pulmonary opacities: plain tomography. *Radiology* 1987; 163: 481–485.
84. Zerhouni EA, Boukadoum M, Siddiky MA, *et al.* A standard phantom for quantitative CT analysis of pulmonary nodules. *Radiology* 1983; 149: 767–773.
85. Ginsberg MS, Griff SK, Go BD, Yoo HH, Schwartz LH, Panicek DM. Pulmonary nodules resected at video-assisted thoracoscopic surgery: etiology in 426 patients. *Radiology* 1999; 213: 277–282.
86. Onitsuka H, Tsukuda M, Araki A, Murakami J, Torii Y, Masuda K. Differentiation of central lung tumor from postobstructive lobar collapse by rapid sequence computed tomography. *J Thorac Imaging* 1991; 6: 28–31.
87. Woodring JH, Johnson PJ. Computed tomography distinction of central thoracic masses. *J Thorac Imaging* 1991; 6: 32–39.
88. Woodring JH. Determining the cause of pulmonary atelectasis: a comparison of plain radiography and CT. *Am J Roentgenol* 1988; 150: 757–763.
89. Byrd RB, Carr DT, Miller WE, Payne WS, Woolner LB. Radiographic abnormalities in carcinoma of the lung as related to histological cell type. *Thorax* 1969; 24: 573–575.
90. Webb WR, Gamsu G, Glazer G. Computed tomography of the abnormal pulmonary hilum. *J Comput Assist Tomogr* 1981; 5: 485–490.
91. Lewis JW Jr, Pearlberg JL, Beute GH, *et al.* Can computed tomography of the chest stage lung cancer? Yes and no. *Ann Thorac Surg* 1990; 49: 591–595.
92. Gdeedo A, Van Schil P, Corthouts B, Van Mieghem F, Van Meerbeeck J, Van Marck E. Comparison of imaging TNM [(i)TNM] and pathological TNM [pTNM] in staging of bronchogenic carcinoma. *Eur J Cardiothoracic Surg* 1997; 12: 224–227.
93. Laroche C, Wells F, Coulden R, *et al.* Improving surgical resection rate in lung cancer. *Thorax* 1998; 53: 445–449.
94. Quint LE, Francis IR. Radiologic staging of lung cancer. *J Thorac Imaging* 1999; 14: 235–246.
95. Glazer HS, Kaiser LR, Anderson DJ, *et al.* Indeterminate mediastinal invasion in bronchogenic carcinoma: CT evaluation. *Radiology* 1989; 173: 37–42.
96. Yokoi K, Mori K, Miyazawa N, Saito Y, Okuyama A, Sasagawa M. Tumor invasion of the chest wall and mediastinum in lung cancer: evaluation with pneumothorax CT. *Radiology* 1991; 181: 147–152.
97. Watanabe A, Shimokata K, Saka H, Nomura F, Sakai S. Chest CT combined with artificial pneumothorax: value in determining origin and extent of tumor. *Am J Roentgenol* 1991; 156: 707–710.
98. Webb WR, Gatsonis C, Zerhouni EA, *et al.* CT and MR imaging in staging non-small cell bronchogenic carcinoma: report of the Radiologic Diagnostic Oncology Group. *Radiology* 1991; 178: 705–713.
99. Piehler JM, Pairolero PC, Weiland LH, Offord KP, Payne WS, Bernatz PE. Bronchogenic carcinoma with chest wall invasion: factors affecting survival following en bloc resection. *Ann Thorac Surg* 1982; 34: 684–691.
100. Murata K, Takahashi M, Mori M, *et al.* Chest wall and mediastinal invasion by lung cancer: evaluation with multisection expiratory dynamic CT. *Radiology* 1994; 191: 251–255.

101. Suzuki N, Saitoh T, Kitamura S. Tumor invasion of the chest wall in lung cancer: diagnosis with US. *Radiology* 1993; 187: 39–42.
102. Heelan RT, Demas BE, Caravelli JF, *et al.* Superior sulcus tumors: CT and MR imaging. *Radiology* 1989; 170: 637–641.
103. McLoud TC, Filion RB, Edelman RR, Shepard JA. MR imaging of superior sulcus carcinoma. *J Comput Assist Tomogr* 1989; 13: 233–239.
104. Pearson FG. Staging of the mediastinum. Role of mediastinoscopy and computed tomography. *Chest* 1993; 103: 346S–348S.
105. Libshitz HI, McKenna RJ Jr. Mediastinal lymph node size in lung cancer. *Am J Roentgenol* 1984; 143: 715–718.
106. Staples CA, Muller NL, Miller RR, Evans KG, Nelems B. Mediastinal nodes in bronchogenic carcinoma: comparison between CT and mediastinoscopy. *Radiology* 1988; 167: 367–372.
107. Dales RE, Stark RM, Raman S. Computed tomography to stage lung cancer. Approaching a controversy using meta-analysis. *Amer Rev Respir Dis* 1990; 141: 1096–1101.
108. McLoud TC, Bourgouin PM, Greenberg RW, *et al.* Bronchogenic carcinoma: analysis of staging in the mediastinum with CT by correlative lymph node mapping and sampling. *Radiology* 1992; 182: 319–323.
109. Investigation for mediastinal disease in patients with apparently operable lung cancer. Canadian Lung Oncology Group. *Annals of Thoracic Surgery* 1995; 60: 1382–1389.
110. Seely JM, Mayo JR, Miller RR, Muller NL. T1 lung cancer: prevalence of mediastinal nodal metastases and diagnostic accuracy of CT. *Radiology* 1993; 186: 129–132.
111. Kirsh MM, Kahn DR, Gago O, *et al.* Treatment of bronchogenic carcinoma with mediastinal metastases. *Annals of Thoracic Surgery* 1971; 12: 11–21.
112. Martini N, Flehinger BJ, Zaman MB, Beattie EJ Jr. Results of resection in non-oat cell carcinoma of the lung with mediastinal lymph node metastases. *Annals of Surgery* 1983; 198: 386–397.
113. Silvestri GA, Littenberg B, Colice GL. The clinical evaluation for detecting metastatic lung cancer. A meta-analysis. *Amer J Respir Crit Care Med* 1995; 152: 225–230.
114. Sider L, Horejs D. Frequency of extrathoracic metastases from bronchogenic carcinoma in patients with normal-sized hilar and mediastinal lymph nodes on CT. *Am J Roentgenol* 1988; 151: 893–895.
115. Grant D, Edwards D, Goldstraw P. Computed tomography of the brain, chest, and abdomen in the preoperative assessment of non-small cell lung cancer. *Thorax* 1988; 43: 883–886.
116. Hillers TK, Sauve MD, Guyatt GH. Analysis of published studies on the detection of extrathoracic metastases in patients presumed to have operable non-small cell lung cancer. *Thorax* 1994; 49: 14–19.
117. Quint LE, Tummala S, Brisson LJ, *et al.* Distribution of distant metastases from newly diagnosed non-small cell lung cancer. *Ann Thorac Surg* 1996; 62: 246–250.
118. Ferrigno D, Buccheri G. Cranial computed tomography as a part of the initial staging procedures for patients with non-small-cell lung cancer. *Chest* 1994; 106: 1025–1029.
119. Salvatierra A, Baamonde C, Llamas JM, Cruz F, Lopez-Pujol J. Extrathoracic staging of bronchogenic carcinoma. *Chest* 1990; 97: 1052–1058.
120. Kormas P, Bradshaw JR, Jeyasingham K. Preoperative computed tomography of the brain in non-small cell bronchogenic carcinoma. *Thorax* 1992; 47: 106–108.
121. Karnofsky DA, Burchenal JH. The clinical evaluation of chemotherapeutic agents in cancer. *In*: Macleod CM, ed. Evaluation of Chemotherapeutic Agents. New York, Columbia University Press, 1949; pp. 199–205.
122. Colice GL, Birkmeyer JD, Black WC, Littenberg B, Silvestri G. Cost-effectiveness of head CT in patients with lung cancer without clinical evidence of metastases. *Chest* 1995; 108: 1264–1271.
123. Earnest F, Ryu JH, Miller GM, *et al.* Suspected non-small cell lung cancer: incidence of occult brain and skeletal metastases and effectiveness of imaging for detection-pilot study. *Radiology* 1999; 211: 37–145.
124. Remer EM, Obuchowski N, Ellis JD, Rice TW, Adelstein DJ, Baker ME. Adrenal mass evaluation in patients with lung carcinoma: a cost-effectiveness analysis. *Am J Roentgenol* 2000; 174: 1033–1039.
125. Gillams A, Roberts CM, Shaw P, Spiro SG, Goldstraw P. The value of CT scanning and percutaneous fine needle aspiration of adrenal masses in biopsy-proven lung cancer. *Clin Radiol* 1992; 46: 18–22.
126. Korobkin M, Lombardi TJ, Aisen AM, *et al.* Characterization of adrenal masses with chemical shift and gadolinium-enhanced MR imaging. *Radiology* 1995; 197: 411–418.
127. Schwartz LH, Panicek DM, Koutcher JA, *et al.* Adrenal masses in patients with malignancy: prospective comparison of echo-planar, fast spin-echo, and chemical shift MR imaging. *Radiology* 1995; 197: 421–425.
128. Erasmus JJ, Patz EF Jr, McAdams HP, *et al.* Evaluation of adrenal masses in patients with bronchogenic carcinoma using 18F-fluorodeoxyglucose positron emission tomography. *Am J Roentgenol* 1997; 168: 1357–1360.
129. Shaffer K. Radiologic evaluation in lung cancer: diagnosis and staging. *Chest* 1997; 112: 235S–238S.
130. Elias AD. Small cell lung cancer: state-of-the-art therapy in 1996. *Chest* 1997; 112: 251S–258S.
131. Klein JS, Salomon G, Stewart EA. Transthoracic needle biopsy with a coaxially placed 20-gauge automated cutting needle: results in 122 patients. *Radiology* 1996; 198: 715–720.
132. Salazar AM, Westcott JL. The role of transthoracic needle biopsy for the diagnosis and staging of lung cancer. *Clin Chest Med* 1993; 14: 99–110.